JCB Journal of Cell Biology

ARTICLE

C-ferroptosis is an iron-dependent form of regulated cell death in cyanobacteria

Anabella Aguilera[1*], Federico Berdun[1*], Carlos Bartoli[2], Charlotte Steelheart[2], Matías Alegre[2], Hülya Bayir[4,5,6,7,8], Yulia Y. Tyurina[7,8], Valerian E. Kagan[6,7,8,9], Graciela Salerno[1], Gabriela Pagnussat[3], and María Victoria Martin[1]

Ferroptosis is an oxidative and iron-dependent form of regulated cell death (RCD) recently described in eukaryotic organisms like animals, plants, and parasites. Here, we report that a similar process takes place in the photosynthetic prokaryote *Synechocystis* sp. PCC 6803 in response to heat stress. After a heat shock, *Synechocystis* sp. PCC 6803 cells undergo a cell death pathway that can be suppressed by the canonical ferroptosis inhibitors, CPX, vitamin E, Fer-1, liproxstatin-1, glutathione (GSH), or ascorbic acid (AsA). Moreover, as described for eukaryotic ferroptosis, this pathway is characterized by an early depletion of the antioxidants GSH and AsA, and by lipid peroxidation. These results indicate that all of the hallmarks described for eukaryotic ferroptosis are conserved in photosynthetic prokaryotes and suggest that ferroptosis might be an ancient cell death program.

Introduction

In contrast with accidental cell death, regulated cell death (RCD) relies on a tightly modulated molecular machinery that involves signaling cascades and defined effectors (Galluzzi et al., 2018). In eukaryotes, RCD plays a critical role in essential physiological programs such as embryonic development, differentiation, fertilization, tissue renewal, and immune responses, generally referred to as programmed cell death (PCD; Hakem et al., 1998; Lindsten et al., 2000; Van Hautegem et al., 2015; Yoshida et al., 1998). RCD can also occur when responses to perturbations of the intracellular or extracellular microenvironment fail, as an ultimate attempt to maintain homeostasis (Galluzzi et al., 2016).

Different types of RCD have been described in eukaryotes (Melino et al., 2005; Minina et al., 2013). Among them, ferroptosis was recently reported as an oxidative, iron-dependent form of RCD characterized by the disturbed thiol homeostasis and the accumulation of lipid hydroperoxides to lethal levels. Ferroptosis is present and relevant in animals, plants, and protozoan parasites (Bogacz and Krauth-Siegel, 2018; Conrad et al., 2018; Distéfano et al., 2017; Dixon et al., 2012; Stockwell et al., 2017). Although less studied and understood, RCD also occurs in prokaryotic microorganisms (Allocati et al., 2015; Bayles, 2014; Dar et al., 2018; Durand et al., 2016).

Cyanobacteria are widely distributed Gram-negative bacteria that are capable of plant-like oxygenic photosynthesis. In particular, cyanobacteria are important components of phytoplankton communities, contributing to a substantial fraction of the global primary production, and are a crucial source of atmospheric oxygen (Whitton, 2012). Despite its ecological and biogeochemical significance, the nature of RCD in cyanobacteria is still not completely understood (Aguilera et al., 2021). Evidence has accumulated on controlled cell death mechanisms triggered in cyanobacteria under unfavorable environmental conditions such as nutrient deprivation, high-light–associated oxidative stress, or osmotic stress, which are indistinctly termed as PCD, apoptotic-like death, or necrotic-like death. Such cell death pathways involve morphological changes, accumulation of reactive oxygen species (ROS), DNA laddering, loss of plasma membrane integrity, and the coordinated participation of redox enzymes, metabolites, and caspase-like proteases (Aguilera et al., 2021; Bidle, 2016; Hu and Rzymski, 2019;

[1]Instituto de Investigaciones en Biodiversidad y Biotecnología (INBIOTEC-CONICET), Fundación para Investigaciones Biológicas Aplicadas (CIB-FIBA), Mar del Plata, Argentina; [2]Instituto de Fisiología Vegetal (INFIVE), Facultades de Ciencias Agrarias y Forestales y de Ciencias Naturales y Museo, Universidad Nacional de La Plata, CCT-CONICET La Plata, La Plata, Argentina; [3]Instituto de investigaciones Biológicas IIB-CONICET, Universidad Nacional de Mar del Plata, Mar del Plata, Argentina; [4]Department of Critical Care Medicine, University of Pittsburgh, Pittsburgh, PA; [5]Safar Center for Resuscitation Research, University of Pittsburgh, Pittsburgh, PA; [6]Children's Neuroscience Institute, University of Pittsburgh, Pittsburgh, PA; [7]Center for Free Radical and Antioxidant Health, University of Pittsburgh, Pittsburgh, PA; [8]Departments of Environmental and Occupational Health, Chemistry, Pharmacology and Chemical Biology, Radiation Oncology, University of Pittsburgh, Pittsburgh, PA; [9]Institute for Regenerative Medicine, IM Sechenov Moscow State Medical University, Moscow, Russia.

*A. Aguilera and F. Berdun contributed equally to this paper; Correspondence to María Victoria Martin: mvmartin@inbiotec-conicet.gob.ar; Gabriela Pagnussat: gpagnussat@mdp.edu.ar; A. Aguilera's present address is Centre for Ecology and Evolution in Microbial Model Systems, Linnaeus University, Kalmar, Sweden; F. Berdun's present address is Instituto de Investigaciones Biológicas IIB-CONICET, Universidad Nacional de Mar del Plata, Mar del Plata, Argentina.

Spungin et al., 2019; Swapnil et al., 2017; Zhou et al., 2020b). RCD has been proposed to optimize differentiation, dynamics, and colony fitness in cyanobacteria (Bar-Zeev et al., 2013; Meeks and Elhai, 2002). In addition, microscopic analyses showed that cyanobacteria symbiotically associated with the water fern *Azolla microphylla* can follow different RCD pathways with characteristics of metazoan apoptosis, autophagy, necrosis, and autolysis (Zheng et al., 2013).

In this work, we examined whether ferroptosis could be relevant to the model cyanobacterium *Synechocystis* sp. PCC 6803 (hereafter *Synechocystis*) under abiotic stresses. We found that *Synechocystis* follows a cell death program in response to heat stress (50°C) that shows biochemical and morphological features that resemble eukaryotic ferroptosis (Conrad et al., 2018; Distéfano et al., 2017; Dixon et al., 2012). This cell death is dependent on iron availability and lipid peroxidation, and it is inhibited by canonical ferroptosis inhibitors. Moreover, cell death is characterized by depletion of glutathione (GSH) and ascorbic acid (AsA), and can be prevented by GSH or AsA addition. Since this pathway is also characterized by specific features, we termed this cell death process cyanobacterial-ferroptosis (c-ferroptosis). Altogether, these results suggest that ferroptosis might be an ancient cell death program. In addition, as chloroplasts originated from the endosymbiosis of cyanobacterial-like organisms, the presence of this iron-dependent oxidative cell death pathway in cyanobacteria also points to the evolutionary origin of the chloroplasts role during plant ferroptosis (Distéfano et al., 2017).

Results

Ferroptosis inhibitors prevented cell death triggered by a 50°C-heat stress in cyanobacteria

To examine whether ferroptosis plays a role during stress-induced cell death in *Synechocystis*, cells were exposed to different treatments: (1) H_2O_2, known to promote cell death in a regulated way in the cyanobacterium *Microcystis aeruginosa* (Ding et al., 2012; Zhou et al., 2020b); (2) 50°C for 10 min (50°C-heat stress [HS]), known to cause cell death in *Synechocystis* (Suginaka et al., 1999); and (3) 77°C for 10 min, a treatment known to trigger unregulated necrosis in plant roots (Distéfano et al., 2017). Each treatment was applied in the presence or absence of two canonical ferroptosis inhibitors: the lipophilic antioxidant ferrostatin-1 (Fer-1) or the membrane-permeable iron chelator ciclopirox olamine (CPX; Stockwell and Jiang, 2020). Cell death was assessed by three different methodologies following Nomenclature Committee on Cell Death recommendations (Kroemer et al., 2009): drop tests to measure cell survival (Fig. 1 a), fluorescence microscopy using SYTOX Green as a cell death marker (Fig. 1 b and Fig. S1 a), and fluorescein diacetate (FDA) fluorescence quantification by flow cytometry to assess viability (Fig. 1 c). All experiments indicated that cell death triggered by 50°C is significantly prevented by Fer-1 and by CPX (Fig. 1, a–c), suggesting that the 50°C-HS triggers the ferroptotic cell death pathway. In contrast, neither Fer-1 nor CPX was able to prevent cell death triggered by a higher temperature (77°C) or by H_2O_2. In addition, cell death was significantly prevented when *Synechocystis* cells were exposed to 50°C-HS but were preincubated with the lipophilic antioxidants liproxstatin-1 (Lipro-1) and vitamin E, which are also recognized as ferroptosis inhibitors (Fig. 1 d). Altogether, these results indicate that the response of *Synechocystis* cells to 50°C-HS is specific, and can be prevented by canonical ferroptosis inhibitors such as CPX, Fer-1, Lipro-1, and vitamin E (Dixon and Stockwell, 2019; Kagan et al., 2017; Stockwell and Jiang, 2020).

Role of calcium in the RCD pathway triggered by 50°C in *Synechocystis*

To test the effect of calcium on *Synechocystis*, we exposed cells to 50°C-HS in the presence of $CaCl_2$, EGTA, an extracellular calcium chelator, BAPTA-AM, an intracellular calcium chelator, and a combination of these compounds. 4 h after the treatment, ∼70% of 50°C-HS treated cells were found dead (Fig. 2). Surprisingly, when cotreated with $CaCl_2$, only ∼10% of the 50°C-HS treated cells died, a value comparable to the control (cells that were not exposed to HS, Fig. 2 a). On the other hand, ∼90% of the cells were found dead when treated with EGTA, and less than ∼10% were found dead when EGTA and $CaCl_2$ were added together. These results suggest that extracellular calcium can prevent cell death induced by 50°C-HS (Fig. 2 a). However, neither Fer-1 nor CPX was able to prevent cell death in the presence of EGTA (Fig. 2 b).

Cell death triggered by 50°C was significantly prevented by the addition of the intracellular Ca^{2+} chelator (BAPTA-AM; Fig. 2 a). When 50°C-treated cells were preincubated with CPX and BAPTA-AM, cell death reached ∼70%, a value comparable to 50°C-treated cells without inhibitors (Fig. 2 d). This result can be explained by the fact that iron chelators might increase the levels of intracellular calcium, as observed in human cells (Yalcintepe and Halis, 2016). On the other hand, assays combining Fer-1 and BAPTA-AM prevented cell death similarly to the effect of preincubation with BAPTA-AM alone (Fig. 2 d). These results support the role of Ca^{2+} as a second messenger in this cell death pathway, in which extracellular and intracellular sources might play antagonistic roles.

The 50°C-HS induces depletion of the antioxidants GSH and AsA

Ferroptosis is characterized by an early depletion of GSH in animals, and both GSH and AsA in plants (Distéfano et al., 2017; Dixon et al., 2012; Seiler et al., 2008; Skouta et al., 2014). The exposure of *Synechocystis* cells to 50°C resulted in a decline of GSH and AsA total contents (Fig. 3, a–d). These effects were not prevented by the addition of Fer-1 or CPX, suggesting that GSH and AsA depletion might be an early event in this cell death pathway, as described for plant ferroptosis (Distéfano et al., 2017). The redox status of GSH (percentage of oxidized GSH disulfide [GSSG]) did not show a clear association with the treatments and did not show differences with the addition of Fer-1 or CPX under normal temperature conditions. On the other hand, oxidized AsA content was very low or almost undetectable. Notably, cell death was prevented by preincubation with GSH, AsA, and DTT, suggesting that GSH and AsA depletion is required for HS-induced cell death in *Synechocystis* (Fig. 3, e and f).

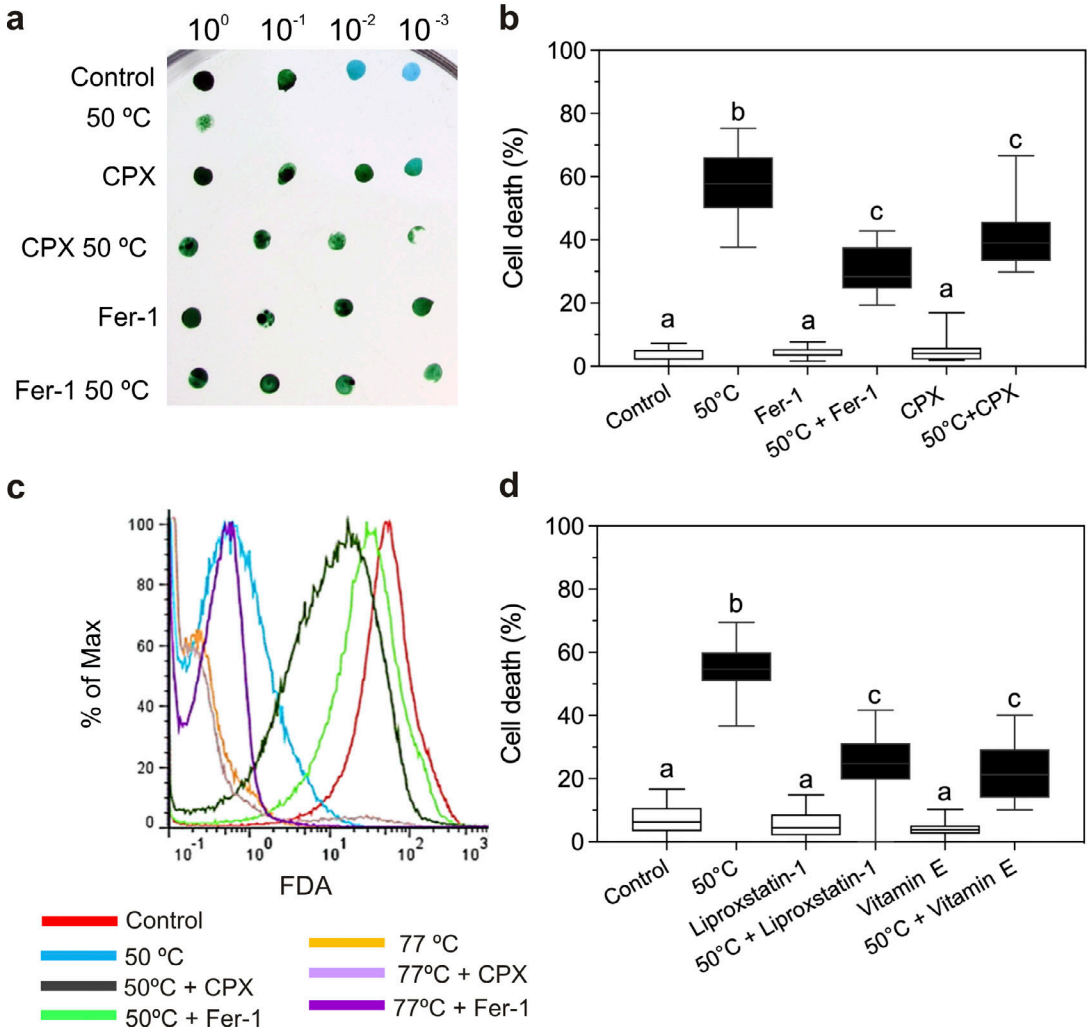

Figure 1. **Ferroptosis inhibitors prevent cell death induced by a 50°C heat shock in *Synechocystis* sp. PCC 6803. (a)** Viability of *Synechocystis* sp. PCC 6803 cells exposed to 50°C for 10 min preincubated with DMSO (-), with Fer-1 (1 µM) or with CPX (1 µM) for 24 h was tested via a drop test on BG11 agar plates. The effect of each treatment was verified by three independent experiments. **(b)** HS-induced cell death in *Synechocystis* sp. PCC 6803 preincubated with DMSO, Fer-1, or CPX for 24 h. **(c)** Cell viability was assessed by flow cytometry using the FDA probe after inducing cell death after a treatment of 50°C or 77°C for 10 min in cultures preincubated with DMSO, Fer-1, or CPX for 24 h. **(d)** HS-induced cell death in *Synechocystis* sp. PCC 6803 preincubated with DMSO, Lipro-1 (5 µM), or vitamin E (500 µM) for 24 h. Cell suspensions were stained with SYTOX Green, examined and counted under light and fluorescence microscopy. SYTOX-positive cells were interpreted as dead cells. Box plots are from at least three independent experiments. Plots with different letters denote statistical difference (two-way ANOVA in GLM, $P < 0.05$). The Shapiro–Wilk test was used to test normal distribution of the residuals.

50°C-HS induced rapid accumulation of cytosolic and lipid ROS

In eukaryotic organisms, lipid ROS accumulation plays a central and essential role in ferroptosis. This oxidative burst is prevented by iron chelators (CPX) and lipophilic antioxidants (Fer-1; Bogacz and Krauth-Siegel, 2018; Distéfano et al., 2017; Dixon et al., 2012). To investigate if a similar process occurs in *Synechocystis*, cytosolic ROS and lipid ROS accumulation were measured after inducing cell death by a 50°C-HS. Cytosolic ROS were measured with the probe H_2DCFDA, while lipid ROS accumulation was monitored with the probe C11-BODIPY. A maximum of cytosolic ROS was detected 1 h after 50°C-HS (Fig. 4 a). This accumulation of cytosolic ROS was prevented by incubation with Fer-1 or CPX (Fig. 4 a). The accumulation of lipid peroxides reached a maximum 3 h after the 50°C-HS and was suppressed by both ferroptosis inhibitors (Fig. 4 b).

Pre-treatments with polyunsaturated fatty acids (PUFAs) deuterated at bis-allylic positions (D-PUFAs) prevent ferroptosis in both human and plant cells (Yang et al., 2016; Distéfano et al., 2017). Likewise, we observed a clear protective effect of D-linoleate (16 h) against the 50°C-HS in *Synechocystis* (Fig. 4 c). Altogether, these results indicate that *Synechocystis* cells exposed to a 50°C-HS undergo an oxidative, iron-dependent form of cell death remarkably similar to ferroptosis in eukaryotic cells (Bogacz and Krauth-Siegel, 2018; Dangol et al., 2019; Distéfano et al., 2017; Dixon et al., 2012).

Redox-lipidomics analysis reveals a lipid oxidation signature of c-ferroptosis

The oxidation of membrane lipids containing PUFAs is one of the main hallmarks that define ferroptosis (Dixon and Stockwell, 2019). To identify the oxygenated lipids that resulted from the

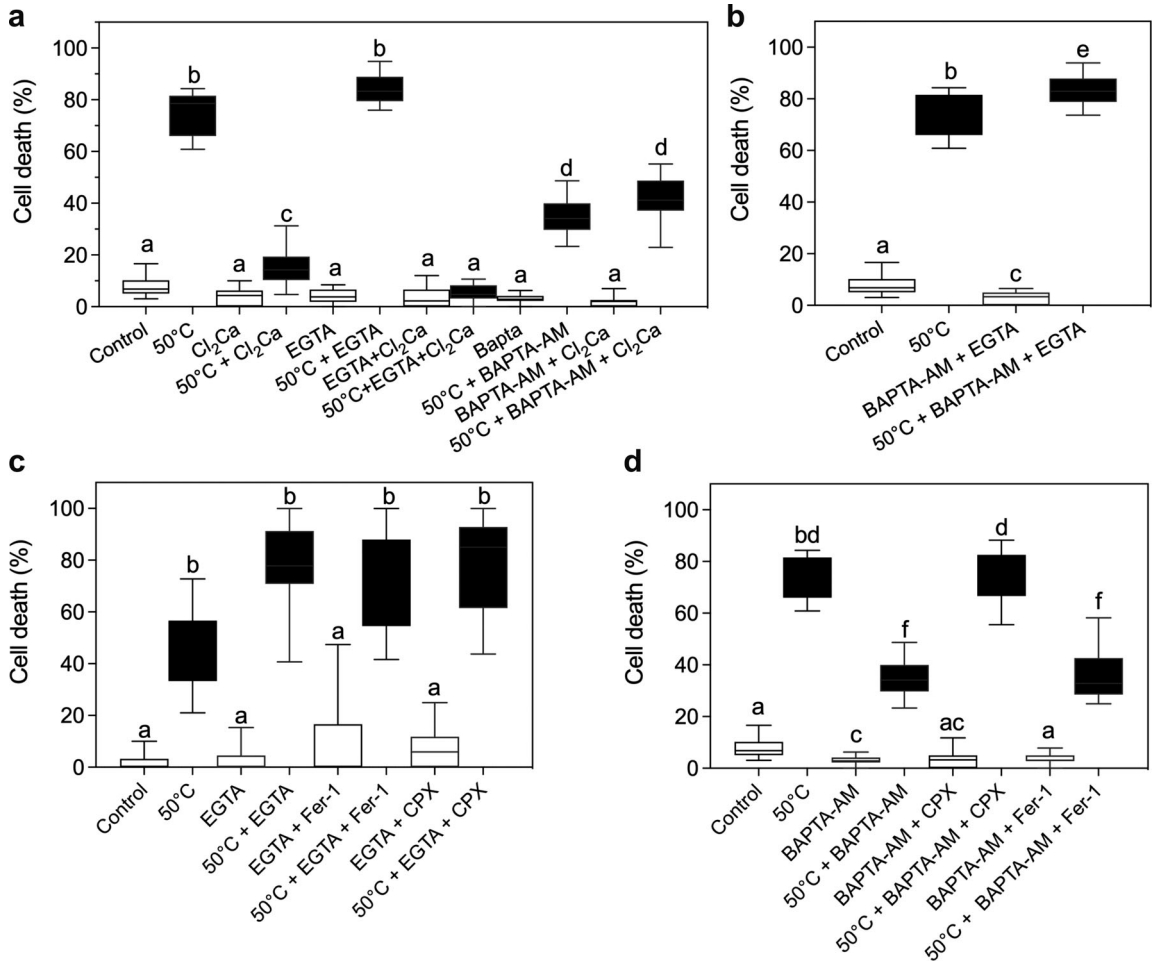

Figure 2. **Exogenous calcium (Ca^{2+}) addition and intracellular Ca^{2+} chelation prevent cell death induced by a 50°C heat shock in *Synechocystis* sp. PCC 6803. (a)** Cell death was assessed in *Synechocystis* sp. PCC 6803 cells preincubated with Cl_2Ca, EGTA, BAPTA-AM, Cl2Ca+BAPTA-AM, or Cl_2Ca+EGTA before inducing cell death by treating cells at 50°C for 4 h. **(b)** Cell death assessed in *Synechocystis* sp. PCC 6803 cells preincubated with EGTA+BAPTA-AM before inducing cell death by treating cells at 50°C for 4 h. **(c)** Cell death assessed in *Synechocystis* sp. PCC 6803 cells preincubated with EGTA and then with Fer-1 or CPX before inducing cell death by treating cells at 50°C for 4 h. **(d)** Cell death assessed in *Synechocystis* sp. PCC 6803 cells preincubated with BAPTA-AM and then with Fer-1 or CPX before inducing cell death by treating cells at 50°C for 4 h. Cell suspensions were stained with SYTOX Green, examined and counted under light and fluorescence microscopy. SYTOX-positive cells were interpreted as dead cells. Box plots are from at least three independent experiments. Plots with different letters denote statistical difference (two-way ANOVA in GLM, $P < 0.05$). The Shapiro–Wilk test was used to test normal distribution of the residuals.

50°C-HS, we performed global redox lipidomics liquid chromatography with tandem mass spectrometry (LC-MS/MS) analysis (Kagan et al., 2017; Tyurin et al., 2008; Tyurina et al., 2014). The 50°C-HS induced the accumulation of oxidized species of phosphatidylethanolamine (PE; 36:4-OO and 36:5-OO) and phosphatidylglycerol (PG; 34:2-O, 34:2-OO, 36:3-OO, 34:3-OO, 36:2-O, and 34:3-O). Interestingly, it also induced the accumulation of oxidized species of the sulfo-lipids sulfoquinovosyl diacylglycerols (SQDGs; 34:2-O, 34:2-OO, 34:4-O, 34:4-OO, and 34:3-O), which are a major component of cyanobacterial thylacoids (Nakajima et al., 2018). Remarkably, this accumulation of oxidized species of phosphor- and sulfo-lipids was prevented when 50°C-treated cells were preincubated with Fer-1, suggesting that they might act as pro-ferroptotic signals in this system (Fig. 5).

In addition, our results indicated that nonoxidized species of the galactolipid monogalactosyldiacylglycerol (MGDG) accumulated when cells were exposed to 50°C (Fig. S2). These lipids are very abundant in the thylakoid membranes and accumulate in response to environmental stress (Yang et al., 2020).

As this pathway seems to be characterized by particular lipid species peroxidation and calcium signaling, we decided to name it c-ferroptosis.

Synechocystis shows thylakoid membranes alteration after heat shock

To gain insight into the morphological changes taking place in our cell death model, *Synechocystis* sp. PCC6803 cells treated with H_2O_2 or subjected to 50°C or to 77°C were studied using transmission EM (TEM; Fig. 6). The distinctive morphological features of 50°C-treated cells involved the loss of the thylakoids membrane integrity, with evident nonelectron dense zones, and vesiculation (Fig. 6). On the other hand, cells exposed to 77°C showed a

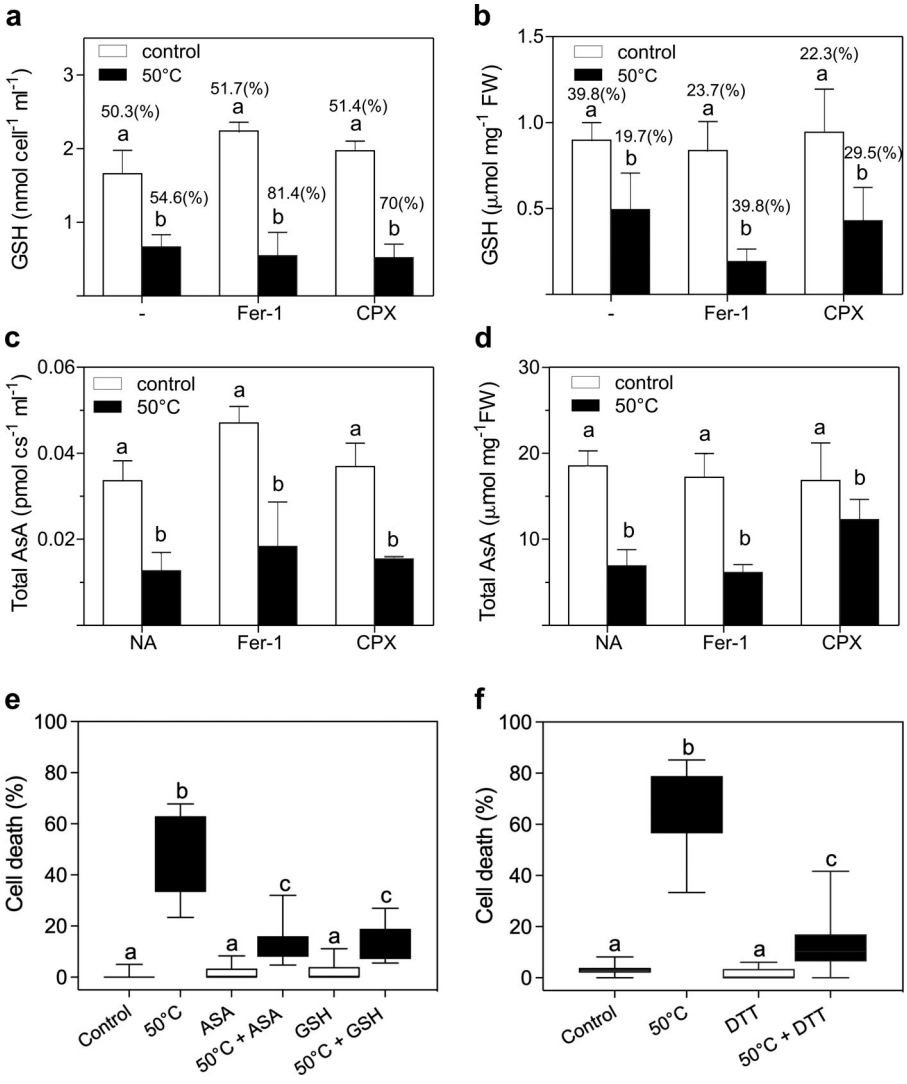

Figure 3. **Cell death triggered by 50°C induces GSH and AsA depletion in *Synechocystis* sp. PCC 6803. (a–c)** GSH and GSSG levels (a and b) and reduced AsA content (b and c) were measured in *Synechocystis* sp. PCC6803 after treating cells at 50°C for 4 h. In each case, preincubation with DMSO (-), Fer-1 (1 µM), or CPX (1 µM) 24 h before HS is indicated. Different letters denote statistical difference (two-way ANOVA, $P < 0.05$). The Shapiro–Wilk test was used to test normal distribution. **(e)** Cell death induced by a 50°C treatment is prevented by GSH (100 µM) or AsA (1 µM) addition 24 h before HS. **(f)** Cell death induced by a 50°C treatment is prevented by DTT (3 mM) addition 24 h before HS. To assess cell death, cell suspensions were stained with SYTOX Green, examined and counted by light and fluorescence microscopy. SYTOX-positive cells were interpreted as dead cells. Box plots with different letters denote statistical difference (two-way ANOVA in GLM, $P < 0.05$). The Shapiro–Wilk test was used to test normal distribution of the residuals. Data shown are from three independent experiments. FW, fresh weight.

reduction of the cellular volume and electron dense regions, while the thylakoid membranes were not distinguishable (Fig. 6). Cells treated with H_2O_2 showed cytoplasm vacuolation (Fig. 6).

Caspase-3/7 activities are not induced after the 50°C-HS in *Synechocystis*

In animals, caspases are a well-studied family of evolutionary conserved cysteine-dependent proteases that are implicated in the regulation of several signaling pathways and are considered as the central executioners of apoptosis (Saraste and Pulkki, 2000; Van Opdenbosch and Lamkanfi, 2019). Plants, protists, fungi, and bacteria lack true caspases but contain various homologues (metacaspases and orthocaspases; Klemenčič and Funk, 2018). Even though several of these homologues have been implicated in stress response and cell death in cyanobacteria, their function and regulation are not yet fully understood (Aguilera et al., 2021; Klemenčič et al., 2019). *Synechocystis* sp. PCC 6803 only contains a single orthocaspase (SyOC), which lacks the catalytic dyad. However, although the protein is presumably proteolytically inactive, the gene is highly expressed (Klemenčič et al., 2019).

We monitored caspase-like activity in treated *Synechocystis* cells by using the CellEvent caspase-3/7 green detection reagent, following previous studies on cell death in cyanobacteria (reviewed by Hu and Rzymski, 2019). Caspase-3/7 signals did not increase after exposing cells to 50°C, 77°C, or H_2O_2 (Fig. S3), suggesting that caspase-like activities might not be involved in the cell death processes induced by these triggers, in accordance with previous reports in animal cells (Dixon et al., 2012).

Molecular mechanisms governing ferroptosis in *Synechocystis*

To gain insight into the regulation of several candidate genes that might be involved in cyanobacteria ferroptosis, we examined their expression after exposing *Synechocystis* cells to a 50°C-HS, preincubated or not with Fer-1 or CPX (Table 1). The genes analyzed include the following. Genes were analyzed that were involved in cyanobacterial GSH synthesis (*gshA* and *gshB*) and GSH catabolism (*ggt*; Narainsamy et al., 2016); and *gpx1* and *gpx2*, orthologues to human GSH peroxidase (GPX4), which is essential for ferroptosis in animals (Friedmann Angeli et al., 2014; Imai et al., 2017). Three genes, *gshA*, *ggt*, and *gpx2*, were up-regulated after 50°C exposure, and only *gpx2* was down-regulated.

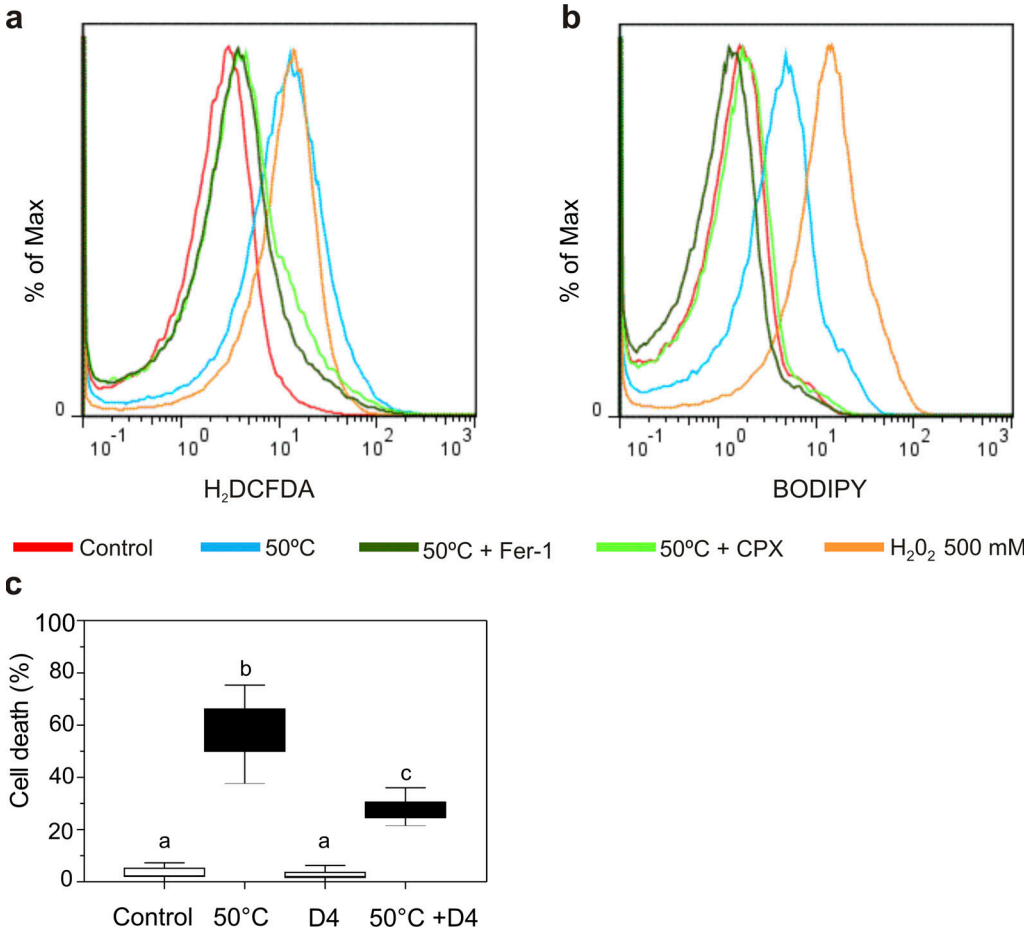

Figure 4. **50°C treatment triggers the accumulation of ROS and lipid ROS. (a and b)** Cytosolic and lipid ROS levels were assessed by flow cytometry at 1 h and 3 h, respectively, after a 10-min 50°C treatment using H_2DCFDA and BODIPY. Cultures were preincubated with DMSO, Fer-1 (1 µM), or CPX (1 µM) for 24 h, as indicated. Aliquots treated with 500 mM H_2O_2 were used as positive controls for ROS content and oxidized lipids production. **(c)** Cell death after 50°C is prevented by D-PUFAs (D4). Cultures were preincubated with DMSO or with 50 µM D4-linoleate for 24 h. Cell death was induced by treating cells at 50°C for 4 h. Cell suspensions were stained with SYTOX Green, examined and counted by light and fluorescence microscopy. SYTOX-positive cells were interpreted as dead cells. Box plots are from three independent experiments. Plots with different letters denote statistical difference (two-way ANOVA in GLM, $P < 0.05$). The Shapiro–Wilk test was used to test normal distribution of the residuals.

On the other hand, *gpx1* and *gshB* were found to be poorly expressed in the analyzed conditions. Only *gpx2* showed a clear response to HS, an induction of ∼10-fold that was prevented by CPX (Table 1). Genes were analyzed that were involved in Fe metabolism such as ferric and ferrous iron transporters (*futA*, *futB*, *futC*, and *feoB*) and the *isiA* gene, which encodes a chlorophyll-binding protein inducible by high light (Havaux et al., 2005). *feoB* was highly up-regulated after the 50°C-HS, which was enhanced by the pretreatment with Fer-1 (Table 1). Genes were analyzed that were related to the heat shock regulon involved in heat stress (*groES*, *groEL*; Rajaram et al., 2014). *GroES* and *groEL* were up-regulated after HS, and that was not prevented by pretreatment with ferroptosis inhibitors (Table 1).

Discussion

Altogether, our results demonstrate that an iron-dependent, oxidative type of cell death takes place in a photosynthetic prokaryote (cyanobacteria) in response to heat stress. Notably, several hallmarks that characterize ferroptosis in animals and ferroptosis-like in plants (Distéfano et al., 2017; Dixon and Stockwell, 2019) are conserved in this cyanobacterial pathway.

Synechocystis cell death triggered by 50°C-HS is prevented by the canonical ferroptosis inhibitors CPX, Fer-1, Lipro-1, and vitamin E (Dixon and Stockwell, 2019; Kagan et al., 2017; Stockwell and Jiang, 2020). While CPX is a membrane-permeable iron chelator, the other ferroptosis inhibitors act by preventing the production of lipid hydroperoxides, which are the ultimate pro-ferroptotic signals (Friedmann Angeli et al., 2014; Kagan et al., 2017; Stockwell and Jiang, 2020; Anthonymuthu et al., 2021).

Lipid ROS accumulation can also be prevented by supplementing cells with bis-allylic deuterated PUFAs, which are less susceptible to peroxidation (Bogacz and Krauth-Siegel, 2018; Distéfano et al., 2017). Cell death in *Synechocystis* was significantly reduced when cells were preincubated with deuterated PUFAs, as seen in eukaryotes (Figs. 3 and 4). PUFAs are present in cyanobacteria as part of phospho- and sulfo-lipids in the membranes of thylakoids. Several stress conditions such as high temperature, high light, or algaecide exposure have been shown

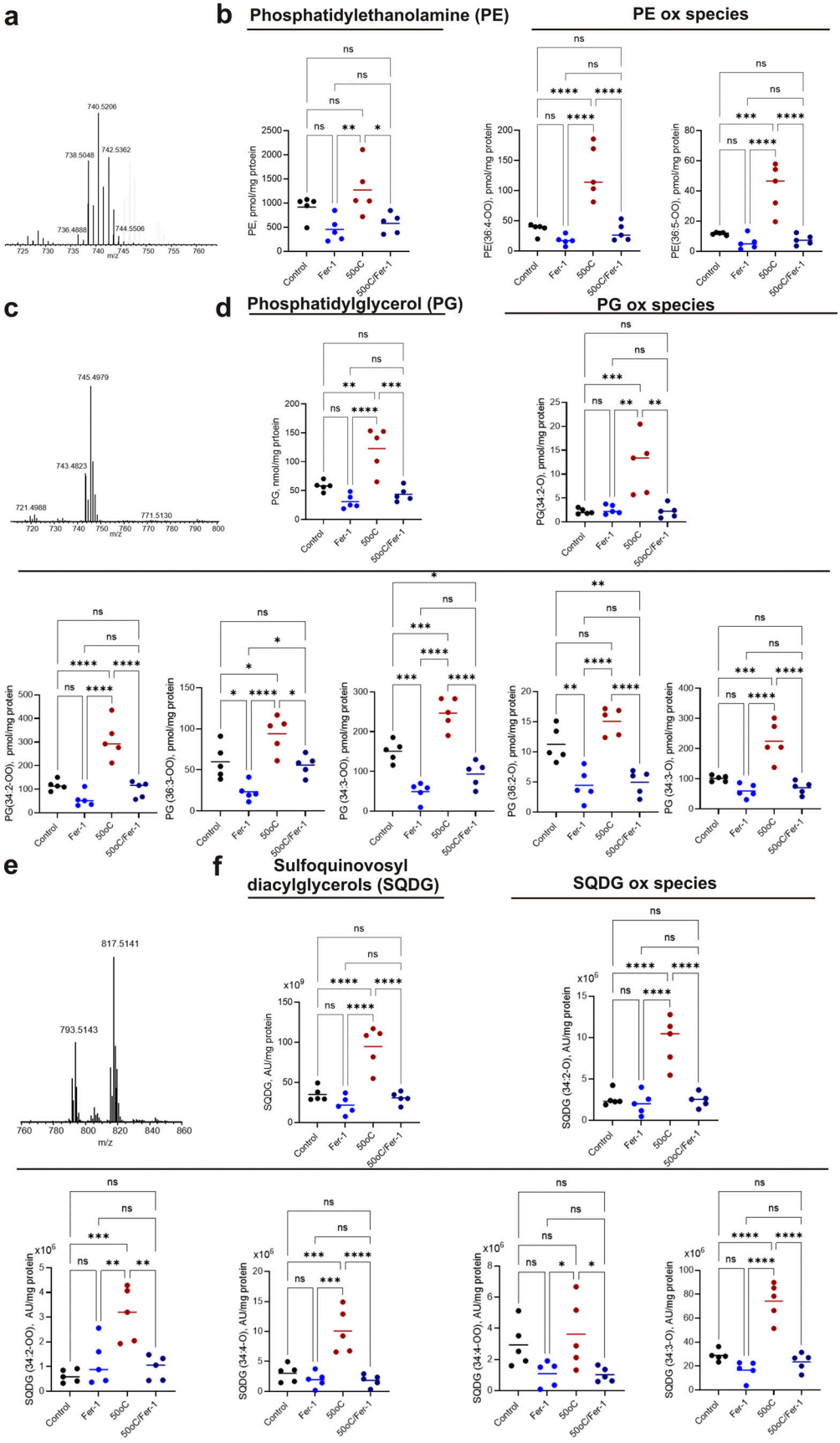

Figure 5. **Oxidized species of PE, PG, and SQDG are accumulated in response to HS.** Quantitative assessments of oxidized (ox) lipid species generated in *Synechocystis* sp. PCC 6803 cells exposed to HS and the ferroptosis inhibitor Fer-1. **(a)** Typical mass spectrum of PE found in cyanobacteria acquired in negative

mode. Separation of lipid was performed by using normal phase chromatography. **(b)** Accumulation of PE and oxidized species of PE observed in *Synechocystis* cells in response to HS with or without treatment with Fer-1. **(c)** Typical mass spectrum of PG in cyanobacteria acquired in negative mode. Separation of lipid was performed by using normal phase chromatography. **(d)** Accumulation of PG oxidized species of PG observed in *Synechocystis* cells in response to HS with or without treatment with Fer-1. **(e)** Typical mass spectrum of SQDG in cyanobacteria acquired in negative mode. Separation of lipid was performed by using normal phase chromatography. **(f)** Content of SQDGs and oxidized species of SQDG in *Synechocystis* cells in response to HS with or without treatment with Fer-1. *, $P < 0.05$ versus control; **, $P < 0.05$ versus ΔwspF (one-way ANOVA); $n = 5$. The accumulation of oxidized species of PE, PG, and SQDG observed in response to HS is prevented by Fer-1 treatment.

to trigger the generation of lipid peroxides (Allakhverdiev et al., 1999; Latifi et al., 2009; Lee et al., 2018; Maeda et al., 2005; Singh et al., 2002). Oxidation of PUFA-containing phospholipids by lipoxygenases (LOXs; encoded by the ALOX genes) is a likely mechanism required contributing to the execution of ferroptotic cell death in mammalian cells (Yang et al., 2016). Several LOX sequences have been detected in cyanobacteria from the genera *Anabaena*, *Nostoc*, *Microcystis*, and *Synechococcus*, and a mini-LOX has been biochemically characterized in *Cyanothece* (Andreou et al., 2010; Hansen et al., 2013; Table 2). However, the biological role of bacterial LOXs remains to be elucidated (Hansen et al., 2013), with the notable exception of 15-LOX from a Gram-negative bacterial pathogen, *Pseudomonas aeruginosa*, that oxidizes host arachidonoyl-PE and triggers "theft-ferroptopsis" in a variety of mammalian cells (Dar et al., 2018).

Long-chain acyl-CoA synthetase-4 (ACSL4) modulates the metabolic fates of PUFAs in human and mouse cells. Remarkably, the deletion of the ACSL4 gene causes resistance to ferroptosis in mammals (Doll et al., 2017). The *Synechocystis* genome includes a sequence that encodes a putative acyl-acyl carrier protein synthetase (SynAas, Slr1609) that is a homologue of the *Arabidopsis thaliana* long-chain acyl-CoA synthetase 9 (LACS9; Table 2). SynAas specifically uses acyl-acyl carrier protein as a cosubstrate to recycle free fatty acids and it is also involved in the transfer of free fatty acids across membranes by vectorial acylation (Kaczmarzyk and Fulda, 2010; von Berlepsch et al., 2012). slr1609-knockout mutants are not able to import exogenous fatty acids as well as fatty acids secreted from membrane lipids into the culture medium (Kaczmarzyk and Fulda, 2010), highlighting the role of SynAas in recycling fatty acids. Further studies are required to evaluate whether SynAas deletion prevents ferroptosis in *Synechocystis* as well.

Lipidomic studies have identified oxidized arachidonic/adrenic PEs as pro-ferrototic signals in human cells (Kagan et al., 2017). While in general prokaryotes membranes contain saturated or monounsaturated lipids, the inner membranes of tylakoids contain MGDGs, digalactosyldiacylglycerols, SQDGs, PGs, and PEs with fatty acyl substituents with a variable number of carbon atoms and a high degree of unsaturation (Hewelt-Belka et al., 2020; Wada and Murata, 1998).

Our results demonstrating the Fer-1–inhibitable accumulation of oxidized species of PE, PG, and SQDG in response to HS strongly suggest that these oxidized species might act as pro-ferroptosis signals in cyanobacteria. Remarkably, we found that when cyanobacteria were exposed to 50°C, the cells clearly showed a loss of the thylakoids membrane integrity, with evident nonelectron dense zones, and vesiculation. Notably, these features are already known to occur after heat treatment in plants (Ristic et al., 2007) and in the unicellular eukaryotic algae

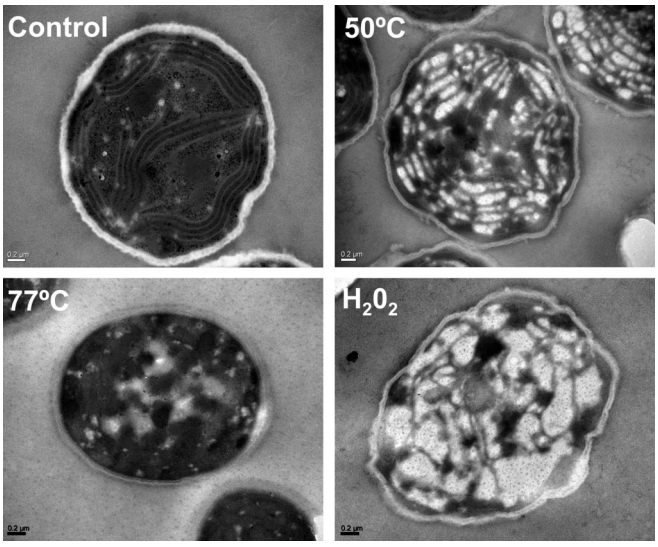

Figure 6. **Morphological studies of *Synechocystis* sp. PCC 6803 under heat and oxidative stress.** TEM micrographs of *Synechocystis* sp. PCC 6803 cells. Cultures were treated with DMSO (control), 50°C, or 77°C for 10 min or with H_2O_2 10 mM for 1 h.

Table 1. **Changes in expression of candidate genes potentially associated with ferroptosis in *Synechococcus* sp. PCC 6803 30 min after a 50°C treatment for 1 h**

Gene	Treatment		
	50°C	50°C + Fer-1	50°C + CPX
groEL1	18.9 ± 9.5	17.9 ± 9.1	12.1 ± 2.5
groES	13.2 ± 7.5	13.3 ±1.1	13.9 ± 1.2
gshA	11.7 ± 0.6	34.0 ±7.0	11.3 ± 5.1
gshB	0.9 ± 0.0	2.3 ± 0.7	0.4 ± 0.4
ggt	4.00 ± 0.9	8.5 ± 4.6	3.0 ± 1.5
gpx1	0.3 ± 0.2	0.2 ± 0.1	0.2 ± 0.1
gpx2	10.0 ± 0	10.0 ± 0	n.d.
feoB	42.3 ± 12.1	79.7 ± 17.0	25.0 ± 9.5
furA	0.6 ± 0.1	1.0 ± 0.1	0.5 ± 0.3
futA	4.3 ± 0.6	10.7 ± 5.7	3.0 ± 1.0
futB	2.8 ± 0.7	7.4 ± 3.4	2.2 ± 0.9
futC	0.7 ± 0.0	2.2 ± 1.5	0.5 ± 0.4

The levels of mRNA are expressed as a fold-change ratio between the treatment and its control condition (cells not exposed to 50°C). n.d., not determined.

Table 2. **Components of the eukaryotic ferroptosis pathway found in cyanobacteria**

Gene/metabolite/process	Cyanobacteria
Selenium-containing GSH peroxidase 4 (GPX4)	The genome of *Synechocystis* sp. PCC 6803 encodes two gpx-like proteins annotated as GPX1 (slr1171) and GPX2 (slr1992) with high similarity to higher plants and mammals. In vitro experiments show that they use unsaturated fatty acid hydroperoxides or alkyl hydroperoxides as electron acceptors (Gaber et al., 2001).
FSP1–ubiquinol Dihydroorotate dehydrogenase–ubiquinol	*Synechocystis sp.* PCC 6803 encodes one dihydroorotate dehydrogenase (slr1418) that catalyzes the conversion of dihydroorotate to orotate with quinone or plastoquinone as electron acceptor (Nara et al., 2000; Baers et al., 2019).
SLC7A11 transmembrane protein, a key component of the cystine/glutamate transporter system xc^-	Unknown. BlastP searches using cystine/glutamate transporter [Q9UPY5 (XCT_HUMAN)] as query against cyanobacterial genomes retrieved amino acid permeases (this work).
GSH	Key antioxidant involved in the protection against ROS (Latifi et al., 2009). Cell death induced by heat (50°C) is correlated with GSH content in *Synechocystis* sp. PCC 6803 (Suginaka et al., 1999; this work). External addition of GSH prevents cell death in cultures exposed to heat (50°C; this work).
ACSL4	Unknown. Acyl-acyl carrier protein synthetaseof *Synechocystis sp.* PCC 6803 (SynAas, Slr1609, homologue of *Arabidopsis* LACS9) recycles free fatty acids, and it is also involved in the transfer of free fatty acids across membranes by vectorial acylation (Kaczmarzyk and Fulda, 2010; von Berlepsch et al., 2012).
PUFAs	Generally present in cyanobacterial membranes. The unsaturation of fatty acids in membrane lipids enhances the tolerance to salt stress and is essential for low temperature tolerance in *Synechocystis* sp. PCC 6803 (Allakhverdiev et al., 1999; Singh et al., 2002). Cell death induced by heat (50°C) is prevented by supplementation with deuterated PUFAs (this work).
Lipid peroxidation	Measured in several cyanobacteria under stress conditions (Maeda et al., 2005; Latifi et al., 2009; Lee et al., 2018).
LOXs	Unknown. Genes with homology to LOXs (ALOX genes) have been found in some cyanobacteria (Hansen et al., 2013).
Vitamin E (α-tocopherol)	Tocopherols have a role in protecting *Synechocystis* sp. PCC 6803 from lipid peroxidation and high light stress (Maeda et al., 2005).
Autophagy	Cyanobacteria have approximately 10 homologues of autophagy genes, which suggests the prokaryotic origin of some autophagy-related proteins (Yang et al., 2016).

Several key genes, metabolites, and processes relevant to ferroptosis described in humans (Dixon et al., 2012; Conrad et al., 2018) are shown as well as a summary of their potential role in cyanobacteria.

Chlorella saccharophila during cell death induced by heat (Zuppini et al., 2007).

The high levels of vacuolization observed in *Synechocystis* cells after exposure to 50°C for 10 min (Fig. 6) could be due to an increase in the autophagic flux. Ferroptosis has been described as an autophagy-dependent process in animal systems (Zhou et al., 2020a). While autophagy is present in almost all eukaryotes, little is known about whether this process occurs in cyanobacteria. Most prokaryotes have three or four homologues of autophagy genes, but cyanobacteria carry approximately 10 homologues (Yang et al., 2017; Table 2). Notably, it was reported that endosymbiotic cyanobacteria present in the fern *A. microphylla* exhibit autophagy-like cell death that is characterized by a gradual condensation and degradation of the cytoplasm and high levels of vacuolization (Zheng et al., 2013). These observations suggest that autophagy might also be a part of the ferroptotic mechanism in cyanobacteria, although more studies are needed to establish if that is the case.

Eukaryotic ferroptosis is highly linked to GSH metabolism and content (Dixon and Stockwell, 2019). In cyanobacteria, GSH is a key antioxidant involved in the protection against several ROSs (Latifi et al., 2009). In this work, we showed that cell death induced by 50°C was preceded by the depletion of the antioxidants GSH and AsA (Fig. 3, a–d), as reported previously for *Synechocystis* (Suginaka et al., 1999), mammalian cells, and root hairs of *A. thaliana* (Distéfano et al., 2017; Dixon and Stockwell, 2019; Yang and Stockwell, 2016). Moreover, cell death was prevented by preincubation with GSH, AsA, and DTT, suggesting that GSH and AsA depletion is required for HS-induced cell death in *Synechocystis* (Fig. 3, e and f). In mammalian cells, GSH depletion results in the inactivation of the selenoenzyme GPX4, which in turn causes an overwhelming accumulation of lipid peroxides that triggers ferroptosis (Dixon et al., 2012; Seiler et al., 2008; Skouta et al., 2014). Similarly, ferroptosis-like death in plants is characterized by the early depletion of GSH and AsA (Distéfano et al., 2017) as also observed in cyanobacteria (Fig. 3). However, the mechanisms through which GSH is depleted in plants and cyanobacteria are not yet well understood. GSH depletion in eukaryotes can be explained by its extensive consumption in the ER lumen to repair disulfides formed as a consequence of high temperatures (Distéfano et al., 2017; Ozgur et al., 2014). Although cyanobacteria lack the ER, it was proposed

that the process could be very similar in these organisms (Chatterjee et al., 2020; Narainsamy et al., 2016). Additionally, when GSH pool is depleted, AsA cannot be recycled via the thiol-dependent mechanisms. This can explain the low levels of reduced AsA detected in *Synechocystis* treated with 50°C and in *Arabidopsis* roots after heat stress (Distéfano et al., 2017; Foyer and Noctor, 2011; Noctor et al., 2012; this work).

GPX4 is a key regulator of eukaryotic ferroptosis (Seibt et al., 2019; Yang et al., 2014). The genome of *Synechocystis* encodes two GPX-like proteins annotated as GPX1 (*slr1171*) and GPX2 (*slr1992*), which display high similarity to GPXs of angiosperms and mammals that do not contain selenium (Gaber et al., 2001; Table 2). In vitro experiments have shown that recombinant GPX-like proteins of *Synechocystis* can reduce unsaturated fatty acids using NADPH, but they are unable to use GSH as an electron donor (Gaber et al., 2001). However, cyanobacteria have multiple detoxifying enzymes to manage oxidative stress, such as GSH peroxidases and peroxiredoxins (Johnson and Hug, 2019), that might also be involved in this response. The redox network in plants and cyanobacteria is composed of several specific reductases that transfer electrons to either GSH or thioredoxins (Buchanan and Luan, 2005; Müller-Schüssele et al., 2021; Pérez-Pérez et al., 2009). Thus, GPXs in cyanobacteria could use thioredoxins as electron donors, as seen in plants (Gaber et al., 2012).

An alternative system that suppresses phospholipid peroxidation and confers protection against ferroptosis independently from GPX4 and GSH has been recently described in mammalians cells (Doll et al., 2019; Mao et al., 2021). The flavoprotein apoptosis-inducing factor mitochondria-associated 2 (renamed ferroptosis suppressor protein 1 [FSP1]) is a NAD(P)H-dependent oxidoreductase involved in cellular oxidative stress response that counteracts ferroptosis by generating ubiquinol from ubiquinone (also known as coenzyme Q10; Doll et al., 2019). In addition, the enzyme dihydroorotate dehydrogenase was shown to convert ubiquinone to ubiquinol exclusively in mitochondria, helping to combat the effects of lipid peroxidation in a mechanism that resembles the FSP1 system in the plasma membrane (Mao et al., 2021). In plants, plastoquinone and ubiquinone are electron transporters in the electron transport chain of photosynthesis and the aerobic respiratory chain, respectively. Importantly, their reduced forms (plastoquinol and ubiquinol) act as radical scavenging antioxidants to prevent lipid peroxidation, protein oxidation, and DNA damage in the plant response to biotic and abiotic stresses (Havaux, 2020; Liu and Lu, 2016). Although less studied, some components of the photosynthetic electron transport chain have been shown to be important for tolerating oxidative stress in cyanobacteria (Latifi et al., 2009). Plastoquinone is present in cyanobacterial thylakoids and is an essential electron carrier required for photosynthesis and respiration (Mullineaux, 2014). Recent studies suggest that ubiquinol biosynthesis originated in this prokaryotic group (Degli Esposti, 2017). However, it is not known whether plastoquinone or ubiquinone prevents lipid peroxidation in cyanobacteria. On the other hand, the genome of *Synechocystis* encodes one membrane-bound dihydroorotate dehydrogenase (pyrD, *slr1418*) that catalyzes the conversion of dihydroorotate to orotate with quinone or plastoquinone as the electron acceptor (Baers et al., 2019; Nara et al., 2000; Table 2). Further studies are required to elucidate if these enzymes and antioxidants also confer protection against cyanobacterial ferroptosis.

The role of calcium in ferroptosis is still a matter of debate. While the extracellular calcium chelator EGTA was found to block ferroptosis in plants (Distéfano et al., 2017), chelation of extracellular calcium does not prevent cell death in response to GSH depletion in human cancer cells (Dixon et al., 2012). Another report, however, indicates that extracellular calcium influx is required for cell death downstream of GSH depletion in mammalian neuronal-like HT22 cells (Henke et al., 2013). These different behaviors suggest that calcium requirements could be cell type–specific. Calcium is an important second messenger in cyanobacteria and is involved in responses to several stresses such as temperature shock and osmotic stress (Agostoni and Montgomery, 2014). Our studies using calcium chelators and exogenous calcium addition (Fig. 2) suggest that extracellular calcium influx can prevent cell death, in agreement with previous results showing that exogenous Ca^{2+} supplementation improves the tolerance of *Anabaena* sp. PCC 7120 to heat stress (Tiwari et al., 2016). In *Anabaena* sp. PCC7120, a heat shock of 45°C results in a significant increase of intracellular Ca^{2+} levels. Interestingly, the use of Ca^{2+} chelators like EGTA or verapamil, a Ca^{2+} channel blocker, suggests that heat shock mobilizes cytosolic Ca^{2+} from both intracellular and extracellular sources (Torrecilla et al., 2000). However, Ca^{2+} from intracellular reservoirs seems to trigger cell death, as incubation with BAPTA-AM prevents ferroptosis triggered by HS. This role for calcium is in agreement with previous reports in eukaryotic cells, particularly in dopaminergic cells (Do Van et al., 2016), where BAPTA-AM prevents ferroptosis induced by erastin. The accumulation of ROS in the cytosol as a result of HS can not only activate redox-sensitive calcium channels but also trigger Ca^{2+} release from the ER, probably through PLC-induced generation of the second messenger inositol 1,4,5-trisphosphate. The resultant increase in intracellular Ca^{2+} levels affect several aspects of cellular homeostasis, including mitochondrial membrane potential. In conclusion, although our results support a role for Ca^{2+} as a second messenger in c-ferroptosis as occurs in some eukaryotic death pathways (Clapham, 2007; Decrock et al., 2011; Do Van et al., 2016; Ren et al., 2021), the specific sources of intracellular Ca^{2+} and their function in the execution of c-ferroptosis are still unknown.

Concluding remarks

Based on the results obtained in this study, we summarized our current understanding of the pathways leading to ferroptosis in the prokaryote *Synechocystis* (Fig. 7). Concisely, the pathway involves early GSH depletion following an HS, which leads to lipid peroxidation, mostly of PUFA lipids of thylakoid membranes. Canonical ferroptosis inhibitors like the iron chelator ciclopirox CPX, the lipophilic antioxidant Fer-1, Lipro-1, and vitamin E prevent the accumulation of toxic oxidized lipids and cytosolic ROS, inhibiting ferroptotic cell death. Mechanistically, this pathway shows remarkable similarities to eukaryotic

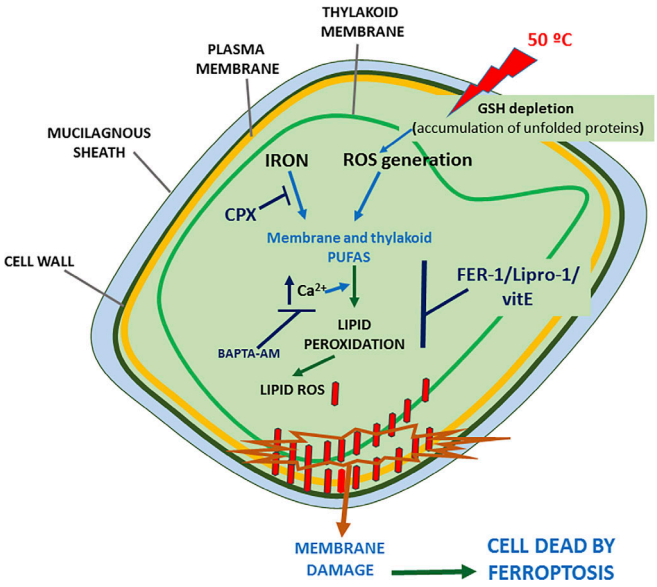

Figure 7. **Schematic view of the c-ferroptotic cell death pathway triggered by heat shock in *Synechocystis* sp. PCC 6803 cells.** Early GSH depletion following the heat shock leads to lipid peroxidation, mostly of PUFAs from thylakoid and plasma membranes. CPX, Lipro-1, vitamin E (vitE), or Fer-1, canonical ferroptosis inhibitors, prevent the accumulation of toxic ROS, inhibiting ferroptotic cell death. Intracellular calcium is a messenger in c-ferroptosis cell death pathways, and BAPTA-AM can suppress this signal and prevent this cell death pathway triggered by heat shock in *Synechocystis* sp. PCC 6803 cells.

ferroptosis. Interestingly, thylakoid membranes seem to be involved in this process, possibly providing PUFA lipids that undergo peroxidation. Thylakoid membranes are enriched in PUFAs, which differentiates cyanobacteria from other prokaryotes, which in general carry membranes containing saturated or monounsaturated lipids (Sharathchandra and Rajashekhar, 2011). This fact can also be related to previous results obtained in the model plant *A. thaliana*, where active chloroplasts were shown to contribute to ferroptotic cell death in leaves (Distéfano et al., 2017).

Altogether, these findings open up a broad field of future research investigating cell death in cyanobacteria, which could be of great relevance in the management of toxic blooms and their ecological consequences.

Materials and methods

Cyanobacterial cells and culture conditions

Axenic cultures of *Synechocystis* sp. PCC 6803 were grown in an orbital shaker (120 rpm) at 28 ± 2°C, under constant light (30 µE m^{-2} s^{-1}) in BG11 medium buffered with 20 mM HEPES-KOH to pH 7.5 (Rippka et al., 1979).

Pre-incubations and heat treatments

Cultures growing in control condition were submitted to heat treatments in a water bath when they reached logarithmic phase (approximately OD_{750} 0.8–0.9). Cells were exposed to 50°C or 77°C for different times (10 min, 30 min, 60 min, 2 h, 4 h, and 6 h). GSH (L-GSH reduced form; Sigma-Aldrich; final concentration 100 µM), AsA (L-AsA; Merck; final concentration 1 µM), D-PUFAs (Retrotope; final concentration 50 µM), CPX (final concentration 1 µM), Fer-1 (final concentration 1 µM), Lipro-1 (final concentration 5 µM) and vitamin E (final concentration 500 µM) were applied to *Synechocystis* sp. PCC 6806 cultures 24 h before the HS. A second pulse of Fer-1 (1 µM) was added 2 h before the HS. For Cl_2Ca, EGTA (extracellular calcium chelator) and BAPTA-AM (intracellular calcium chelator; Torrecilla et al., 2004) experiments, compounds were applied as follows: (1) Cl_2Ca (3 mM final concentration) 24 h before HS; (2) EGTA (1 mM final concentration) 24 h before HS; (3) Cl_2Ca (3 mM) for 2 h followed by addition of EGTA (1 mM) 22 h before HS (Distéfano et al., 2017); and (4) EGTA for 2 h followed by incubation with Fer-1 or CPX for 22 h before inducing cell death by treating cells at 50°C for 4 h. Cultures with no addition were used as controls.

Drop tests for viability analysis

The effect of H_2O_2 (2, 5, and 10 mM for 1 h) and HS (50°C and 77°C for 10 min) in the absence or presence of Fer-1, CPX, GSH, AsA, EGTA, and $CaCl_2$ was tested on solid medium. Serial dilutions of treated cultures were prepared (10^0–10^{-3}), spotted onto solid BG11 agar plates, and cultivated under constant light (30 µE m^{-2} s^{-1}) at 26 ± 2°C for 20 d.

Cell counting and viability determination

Synechocystis cell suspensions were stained with SYTOX Green at a final concentration of 1 µM for 10 min protected from light. Cells were examined and counted by light and fluorescence microscopy using a Nikon E600 microscope equipped with a B-2A cube with 450–490-nm excitation and 500–515-nm emission filters, and a Neubauer chamber. Images were captured by Olympus DP72 digital camera, using Cellsens Entry imaging software. At least 10 random fields were taken for viability calculations in each experiment and quantified in Image J (https://imagej.nih.gov/ij/; Schulze et al., 2011; Fig. S3, a and b).

TEM analysis

Synechocystis cells subjected to H_2O_2 (10 mM for 1 h) and HS (50°C and 77°C for 10 min) were fixed with 2.5% (vol/vol) glutaraldehyde in PBS buffer overnight at 4°C. After washing three times in PBS buffer, samples were post-fixed with 1% (vol/vol) osmium tetroxide in medium buffer for 1 h and washed twice in distilled water. Samples were dehydrated in increasing concentrations of alcohol and embedded in Spurr epoxy. Ultrathin sections (90 nm) were stained in uranyl acetate and lead citrate and examined with a JEM 1200 EX II transmission electron microscope (JEOL Ltd.). Images were captured using a digital camera (Erlangshen ES 1000 W, model 785) from the Central Service of Electron Microscopy of the Faculty of Veterinary Sciences, Universidad Nacional de La Plata (Argentina).

Measurement of GSH and AsA content

50 ml of exponentially growing culture (~2.5 × 10^7 cells ml^{-1}) were collected by centrifugation (9,300 × *g* for 10 min, 4°C), resuspended in 1 ml 3% trifluoracetic acid, mixed thoroughly

(vortexed for 1 min), frozen with liquid nitrogen, thawed in ice, and mixed in vortex for 1 min prior to centrifugation (16,000 × *g* for 15 min, 4°C). Supernatants were passed through a C-18 column (Bond Elute; Varian) for a partial sample purification and eluted in 1 ml 100 mM phosphate buffer, pH 7. Then supernatant was used for GSH and AsA determinations.

The determination of reduced AsA and dehydroascorbate (the oxidized form of AsA) was performed following Aguillera et al. (2020). The content of AsA was determined with a HPLC system using an UV-VIS detector (Model SPD-10AV; Shimadzu) at λ = 265 nm coupled with a LC-10 AT pump (Shimadzu) and compounds separated in a C-18 column (Microsphere C-18 SS 100 × 4.6 mm; Varian Inc.). Results were expressed in picomoles of AsA per cell.

Determination of GSH and GSSG was done following the 5,5′-Dithiobis(2-nitrobenzoic acid) (DTNB) method using GSH reductase and 2-vinylpyridine following Aguillera et al. (2020). Results were expressed in micromoles of GSH or GSSG per cell per mg of fresh weight basis, and in nanomoles per cell.

Flow cytometry experiments

Cell viability, ROS production, lipid peroxidation, and caspase-like activity were assessed by flow cytometry in a Partec Cyflow Space cytometer equipped with a 488-nm laser (blue) and three detectors: 525 nm (green), 590 nm (orange), and 675 nm (red). *Synechocystis* cells in logarithmic phase (OD = 0.8) were used in all the assays.

To test viability, FDA was used as it enters and emits fluorescence only in living cells (Gumbo et al., 2014). An FDA stock solution (1000X) was prepared by solubilizing 50 mg of FDA in 5 ml of DMSO and stored in the dark at −20°C until further use. Cultures pretreated or not with Fer-1 and CPX for 24 h were subjected to 50°C and 77°C for 10 min. After 16 h, cultures were incubated with FDA for 10 min. General cytosolic ROS was measured using H_2DCFDA. A 10 mM H2DCFDA stock solution was prepared in DMSO and stored in the dark at −20°C. BODIPY C-11 581/591 (undecanoic acid) was used for the analysis of lipid peroxidation. This probe detects the oxidation of the polyunsaturated butadienyl portion, changing its emission peak from ∼590 nm to ∼510 nm (Cheloni and Slaveykova, 2013). A 2-mM (1000X) BODIPY stock was prepared and frozen at −20°C. Cultures pretreated or not with Fer-1 or CPX for 24 h were subjected to 50°C and 77°C for 10 min. For ROS and lipid peroxidation analysis, aliquots were taken at different times (30 min, 1 h, 2 h, and 3 h) after HS, incubated with H_2DCFDA or BODIPY for 30 min, and analyzed in the cytometer. Aliquots treated with 500 mM H_2O_2 were used as a positive control for the formation of ROS and oxidized lipids. Caspase-like activity was measure with CellEvent Caspase-3/7 Green Flow Cytometry Assay Kit (Invitrogen), a nucleic acid-binding dye that harbors the caspase-3/7 cleavage sequence, DEVD, and is fluorescent after being cleaved and bound to DNA. Analysis of raw flow cytometry data was done with FlowJo (https://www.flowjo.com/).

Oxidative lipidomics

Lipids were extracted by Folch procedure (Folch et al., 1957) with slight modifications, under nitrogen atmosphere at all steps. LC-electrospray ionization–mass spectrometry (LC/ESI-MS) analysis of lipids was performed on a Dionex HPLC system coupled to an Orbitrap Fusion Lumos mass spectrometer (Thermo Fisher Scientific). Major lipid classes were separated on a normal phase column (Luna 3 µm Silica [2] 100 A; 150 × 1.0 mm; Phenomenex) at a flow rate of 0.050 ml/min. The column was maintained at 35°C. The analysis was performed using gradient solvents as previously described (Sun et al., 2021). To quantitatively assess oxygenated molecular species, lipids were separated on a C30 reverse phase column (Accucore; 2.1 mm × 25 cm; 2.6 µm particle size; Thermo Fisher Scientific). Solvent A was acetonitrile/water (50/50); solvent B was 2-propanol/acetonitile/water (85/10/5). Both A and B solvents contained 5 mM ammonium formate and 0.1% formic acid as modifiers. The gradient method was as follows: 0–40 min, 15–50% B (linear, 5); 40–130 min, 50–100% B (linear, 5); 130–135 min, hold at 100% B; 135–140 min, 15% B (linear, 5); 140–150 min, 15% B for equilibration. The flow was maintained at 100 µl/min. The LC system was a Thermo Ultimate 3000 complete with a WPS-3000 autosampler. Column temperature was set at 35°C. Analysis of LC with mass spectrometry data was performed using software package Compound Discoverer (Thermo Fisher Scientific) with an in-house–generated analysis workflow and lipid database. Lipids were further filtered by retention time and confirmed by fragmentation mass spectrum. Deuterated lipids (Avanti Polar Lipids) were used as internal standards.

RNA isolation and quantitative real-time RT-PCR

Before carrying out our experiments, we examined the expression profiles of our genes of interest (e.g., genes potentially involved in ferroptosis such as cyanobacterial GSH synthesis, Fe metabolism, heat shock response) on expression data (microarray measurements and RNA sequencing) available at CyanoEXpress (http://193.136.227.175/cyanoX/cyanoexpress.html.files/cyanoexpress.intro.html). CyanoEXpress is a web server that enables interactive exploration of curated genome-wide expression data for *Synechocystis* sp. PCC 6803 (Hernandez-Prieto and Futschik, 2012). In particular, we used the RNA sequencing data containing the gene expression of *Synechocystis* sp. PCC 6803 exposed to heat stress of 42°C for 30 min (Kopf et al., 2014). This exploratory analysis showed that several of our genes of interest were up-regulated right after the heat stress. Based on that, we selected the time points to assess gene expression (60 min after the heat shock) in our experiments. Target genes were identified in the genome of *Synechocystis* (http://genome.annotation.jp/cyanobase/Synechocystis), and PCR primers were designed with Primer-BLAST (http://www.ncbi.nlm.nih.gov/tools/primer-blast; Table S1). The analyses of gene expression were performed by real-time quantitative PCR (qPCR). Total RNA was extracted from cell pellets using TRIzol Reagent (Invitrogen) according to the manufacturer's instructions. After digestion with RQ1 RNase-free DNase (Promega), RNA (1 µg) was retro-transcribed using random hexamers (Promega). The qPCR reactions were performed in a Step One real-time PCR system (Applied Biosystems) using a Micro Amp Fast Optical 48-well reaction plate with 15 µl reaction volume containing 1× Power Sybr Green PCR Master Mix (Thermo

Fisher Scientific), 0.2 µM of each primer, and 1.5 µg of cDNA. The cycling program was 1 cycle of 95°C for 10 min, 40 cycles of 95°C for 15 s, and 40 cycles of 54°C for 1 min. A melting curve analysis was conducted to verify the formation of a single unique product and the absence of potential primer dimerization. The different biological samples were subsequently normalized against expression of *rnpB* gene coding for the RNA subunit of RNaseP.

Data analysis

All experiments were performed at least in triplicate. The results are expressed as the mean ± SD. The main effects of treatments were examined by running two-way ANOVA for AsA and GSH data, and two-way ANOVA in generalized linear models (GLMs) module for the rest of the experiments. Binomial distribution was fitted using the *glm* function in R. The Shapiro–Wilk test was used to test whether AsA and GSH data (two-way ANOVA) and residuals for the rest of experiments (two-way ANOVA in GLM) were normally distributed. When significant differences ($P < 0.05$) were found, the Tukey post hoc test was used for multiple comparisons within groups. Statistical analyses were performed using the open access software R (https://www.R-project.org). The ANOVAs of the GLM models and post hoc comparisons were performed with *car* and *lsmeans* packages (Fox and Weisberg, 2010; Lenth, 2016).

Online supplemental material

Fig. S1 presents representative fluorescence images showing cell death in *Synechocystis* sp. PCC 6803. Fig. S2 shows caspase-like activity measured by flow cytometry using CellEvent after 50°C or 77°C for 10 min, or with H_2O_2 10 mM for 1 h. Fig. S3 shows the content of MGDG species in cyanobacteria. Table S1 lists primers used in this study in qPCR reactions.

Acknowledgments

We thank Mikhail S. Shchepinov of Retrotope, Inc., Los Altos, CA, for providing D-PUFAs and Natalia Correa-Aragunde of Instituto de Investigaciones Biológicas-Consejo Nacional de Investigaciones Científicas y Técnicas, Universidad Nacional de Mar del Plata, Mar del Plata, Argentina for providing BAPTA-AM. We would like to thank Silvana Colman, Macarena Perez-Cenci, Gonzalo Caló, Natalia Almada, and Viviana Daniel for technical assistance and Daniela Sueldo and Juan José Guiamet for insightful comments.

This research was funded by grants from Agencia Nacional de Promoción Científica y Técnica Argentina (PICT 1956 and PICT 0173 to M.V. Martin and PICT-2017-0201 to G.C. Pagnussat) and International Centre for Genetic Engineering and Biotechnology (ARG 19-06). A. Aguilera is a postdoctoral fellow of Consejo Nacional de Investigaciones Científicas y Técnicas; F. Berdun is a fellow of Consejo Interuniversitario Nacional. M.V. Martin, G.C. Pagnussat, G. Salerno, and C.G. Bartoli are Consejo Nacional de Investigaciones Científicas y Técnicas researchers.

The authors declare no competing financial interests.

Author contributions: Conceptualization: M.V. Martin, G. Pagnussat, A. Aguilera, F. Berdun, and G. Salerno; methodology: M.V. Martin, G. Pagnussat, A. Aguilera, F. Berdun, C. Bartoli, C. Steelheart, M. Alegre, H. Bayir, Y.Y. Tyurina, and V.E. Kagan; investigation: M.V. Martin, A. Aguilera, F. Berdun, G. Pagnussat, G. Salerno, H. Bayir, Y.Y. Tyurina, and V.E. Kagan; formal analysis: M.V. Martin, A. Aguilera, F. Berdun, G. Pagnussat, H. Bayir, Y.Y. Tyurina, and V.E. Kagan; supervision: M.V. Martin and G. Pagnussat; validation and statistical analysis: M.V. Martin, G. Pagnussat, A. Aguilera, F. Berdun, H. Bayir, Y.Y. Tyurina, and V.E. Kagan; funding acquisition: M.V. Martin and G. Pagnussat; writing of the original draft: M.V. Martin, G. Pagnussat, A. Aguilera, F. Berdun, and G. Salerno; and writing, review, and editing: M.V. Martin, G. Pagnussat, A. Aguilera, F. Berdun, G. Salerno, V.E. Kagan, and C. Bartoli.

Submitted: 1 November 2019
Revised: 29 September 2021
Accepted: 5 November 2021

References

Agostoni, M., and B.L. Montgomery. 2014. Survival strategies in the aquatic and terrestrial world: the impact of second messengers on cyanobacterial processes. *Life (Basel)*. 4:745–769. https://doi.org/10.3390/life4040745

Aguillera, A., C. Steelheart, M. Alegre, F. Berdun, G. Salerno, C. Bartoli, G. Pagnussat, and M.V. Martin. 2020. Measurement of Ascorbic Acid and Glutathione Content in Cyanobacterium *Synechocystis* sp. PCC 6803. *Bio Protoc.* 10:e3800. https://doi.org/10.21769/BioProtoc.3800

Aguilera, A., M. Klemenčič, D.J. Sueldo, P. Rzymski, L. Giannuzzi, and M.V. Martin. 2021. Cell Death in Cyanobacteria: Current Understanding and Recommendations for a Consensus on Its Nomenclature. *Front. Microbiol.* 12:631654. https://doi.org/10.3389/fmicb.2021.631654

Allakhverdiev, S.I., Y. Nishiyama, I. Suzuki, Y. Tasaka, and N. Murata. 1999. Genetic engineering of the unsaturation of fatty acids in membrane lipids alters the tolerance of Synechocystis to salt stress. *Proc. Natl. Acad. Sci. USA.* 96:5862–5867. https://doi.org/10.1073/pnas.96.10.5862

Allocati, N., M. Masulli, C. Di Ilio, and V. De Laurenzi. 2015. Die for the community: an overview of programmed cell death in bacteria. *Cell Death Dis.* 6:e1609. https://doi.org/10.1038/cddis.2014.570

Andreou, A., C. Göbel, M. Hamberg, and I. Feussner. 2010. A bisallylic minilipoxygenase from cyanobacterium Cyanothece sp. that has an iron as cofactor. *J. Biol. Chem.* 285:14178–14186. https://doi.org/10.1074/jbc.M109.094771

Anthonymuthu, T.S., Y.Y. Tyurina, W.-Y. Sun, K. Mikulska-Ruminska, I.H. Shrivastava, V.A. Tyurin, F.B. Cinemre, H.H. Dar, A.P. VanDemark, T.R. Holman, et al. 2021. Resolving the paradox of ferroptotic cell death: Ferrostatin-1 binds to 15LOX/PEBP1 complex, suppresses generation of peroxidized ETE-PE, and protects against ferroptosis. *Redox Biology*. 38: 101744. https://doi.org/10.1016/j.redox.2020.101744

Baers, L.L., L.M. Breckels, L.A. Mills, L. Gatto, M.J. Deery, T.J. Stevens, C.J. Howe, K.S. Lilley, and D.J. Lea-Smith. 2019. Proteome Mapping of a Cyanobacterium Reveals Distinct Compartment Organization and Cell-Dispersed Metabolism. *Plant Physiol.* 181:1721–1738. https://doi.org/10.1104/pp.19.00897

Bar-Zeev, E., I. Avishay, K.D. Bidle, and I. Berman-Frank. 2013. Programmed cell death in the marine cyanobacterium Trichodesmium mediates carbon and nitrogen export. *ISME J.* 7:2340–2348. https://doi.org/10.1038/ismej.2013.121

Bayles, K.W. 2014. Bacterial programmed cell death: making sense of a paradox. *Nat. Rev. Microbiol.* 12:63–69. https://doi.org/10.1038/nrmicro3136

Bidle, K.D. 2016. Programmed cell death in unicellular phytoplankton. *Curr. Biol.* 26:R594–R607. https://doi.org/10.1016/j.cub.2016.05.056

Bogacz, M., and R.L. Krauth-Siegel. 2018. Tryparedoxin peroxidase-deficiency commits trypanosomes to ferroptosis-type cell death. *eLife.* 7:e37503. https://doi.org/10.7554/eLife.37503

Buchanan, B.B., and S. Luan. 2005. Redox regulation in the chloroplast thylakoid lumen: a new frontier in photosynthesis research. *J. Exp. Bot.* 56: 1439–1447. https://doi.org/10.1093/jxb/eri158

Chatterjee, A., K. Rajarshi, H. Ghosh, M.K. Singh, O.P. Roy, and S. Ray. 2020. Molecular chaperones in protein folding and stress management in

cyanobacteria. *In* Advances in Cyanobacterial Biology. P.K. Singh, A. Kumar, V.K. Singh, and A.K. Shrivastava, editors. Academic Press. Cambridge, MA. 119–128. https://doi.org/10.1016/B978-0-12-819311-2.00008-5

Cheloni, G., and V.I. Slaveykova. 2013. Optimization of the C11-BODIPY(581/591) dye for the determination of lipid oxidation in Chlamydomonas reinhardtii by flow cytometry. *Cytometry A.* 83:952–961. https://doi.org/10.1002/cyto.a.22338

Clapham, D.E. 2007. Calcium signaling. *Cell.* 131:1047–1058. https://doi.org/10.1016/j.cell.2007.11.028

Conrad, M., V.E. Kagan, H. Bayir, G.C. Pagnussat, B. Head, M.G. Traber, and B.R. Stockwell. 2018. Regulation of lipid peroxidation and ferroptosis in diverse species. *Genes Dev.* 32:602–619. https://doi.org/10.1101/gad.314674.118

Dangol, S., Y. Chen, B.K. Hwang, and N.-S. Jwa. 2019. Iron- and reactive oxygen species-dependent ferroptotic cell death in rice-Magnaporthe oryzae interactions. *Plant Cell.* 31:189–209. https://doi.org/10.1105/tpc.18.00535

Dar, H.H., Y.Y. Tyurina, K. Mikulska-Ruminska, I. Shrivastava, H.-C. Ting, V.A. Tyurin, J. Krieger, C.M. St Croix, S. Watkins, E. Bayir, et al. 2018. Pseudomonas aeruginosa utilizes host polyunsaturated phosphatidylethanolamines to trigger theft-ferroptosis in bronchial epithelium. *J. Clin. Invest.* 128:4639–4653. https://doi.org/10.1172/JCI99490

Decrock, E., M. Vinken, M. Bol, K. D'Herde, V. Rogiers, P. Vandenabeele, D.V. Krysko, G. Bultynck, and L. Leybaert. 2011. Calcium and connexin-based intercellular communication, a deadly catch? *Cell Calcium.* 50:310–321. https://doi.org/10.1016/j.ceca.2011.05.007

Degli Esposti, M. 2017. A Journey across Genomes Uncovers the Origin of Ubiquinone in Cyanobacteria. *Genome Biol. Evol.* 9:3039–3053. https://doi.org/10.1093/gbe/evx225

Ding, Y., N. Gan, J. Li, B. Sedmak, and L. Song. 2012. Hydrogen peroxide induces apoptotic-like cell death in Microcystis aeruginosa (Chroococcales, Cyanobacteria) in a dose-dependent manner. *Phycologia.* 51:567–575. https://doi.org/10.2216/11-107.1

Distéfano, A.M., M.V. Martin, J.P. Córdoba, A.M. Bellido, S. D'Ippólito, S.L. Colman, D. Soto, J.A. Roldán, C.G. Bartoli, E.J. Zabaleta, et al. 2017. Heat stress induces ferroptosis-like cell death in plants. *J. Cell Biol.* 216:463–476. https://doi.org/10.1083/jcb.201605110

Dixon, S.J., and B.R. Stockwell. 2019. The hallmarks of ferroptosis. *Annu. Rev. Cancer Biol.* 3:35–54. https://doi.org/10.1146/annurev-cancerbio-030518-055844

Dixon, S.J., K.M. Lemberg, M.R. Lamprecht, R. Skouta, E.M. Zaitsev, C.E. Gleason, D.N. Patel, A.J. Bauer, A.M. Cantley, W.S. Yang, et al. 2012. Ferroptosis: an iron-dependent form of nonapoptotic cell death. *Cell.* 149:1060–1072. https://doi.org/10.1016/j.cell.2012.03.042

Do Van, B., F. Gouel, A. Jonneaux, K. Timmerman, P. Gelé, M. Pétrault, M. Bastide, C. Laloux, C. Moreau, R. Bordet, et al. 2016. Ferroptosis, a newly characterized form of cell death in Parkinson's disease that is regulated by PKC. *Neurobiol. Dis.* 94:169–178. https://doi.org/10.1016/j.nbd.2016.05.011

Doll, S., B. Proneth, Y.Y. Tyurina, E. Panzilius, S. Kobayashi, I. Ingold, M. Irmler, J. Beckers, M. Aichler, A. Walch, et al. 2017. ACSL4 dictates ferroptosis sensitivity by shaping cellular lipid composition. *Nat. Chem. Biol.* 13:91–98. https://doi.org/10.1038/nchembio.2239

Doll, S., F.P. Freitas, R. Shah, M. Aldrovandi, M.C. da Silva, I. Ingold, A. Goya Grocin, T.N. Xavier da Silva, E. Panzilius, C.H. Scheel, et al. 2019. FSP1 is a glutathione-independent ferroptosis suppressor. *Nature.* 575:693–698. https://doi.org/10.1038/s41586-019-1707-0

Durand, P.M., S. Sym, and R.E. Michod. 2016. Programmed cell death and complexity in microbial systems. *Curr. Biol.* 26:R587–R593. https://doi.org/10.1016/j.cub.2016.05.057

Folch, J., M. Lees, and G.H. Sloane Stanley. 1957. A simple method for the isolation and purification of total lipides from animal tissues. *J. Biol. Chem.* 226:497–509. https://doi.org/10.1016/S0021-9258(18)64849-5

Fox, J., and S. Weisberg. 2010. An R Companion to Applied Regression. Second edition. SAGE Publications, Inc., Thousand Oaks, CA.

Foyer, C.H., and G. Noctor. 2011. Ascorbate and glutathione: the heart of the redox hub. *Plant Physiol.* 155:2–18. https://doi.org/10.1104/pp.110.167569

Friedmann Angeli, J.P., M. Schneider, B. Proneth, Y.Y. Tyurina, V.A. Tyurin, V.J. Hammond, N. Herbach, M. Aichler, A. Walch, E. Eggenhofer, et al. 2014. Inactivation of the ferroptosis regulator Gpx4 triggers acute renal failure in mice. *Nat. Cell Biol.* 16:1180–1191. https://doi.org/10.1038/ncb3064

Gaber, A., M. Tamoi, T. Takeda, Y. Nakano, and S. Shigeoka. 2001. NADPH-dependent glutathione peroxidase-like proteins (Gpx-1, Gpx-2) reduce unsaturated fatty acid hydroperoxides in Synechocystis PCC 6803. *FEBS Lett.* 499:32–36. https://doi.org/10.1016/S0014-5793(01)02517-0

Gaber, A., T. Ogata, T. Maruta, K. Yoshimura, M. Tamoi, and S. Shigeoka. 2012. The involvement of Arabidopsis glutathione peroxidase 8 in the suppression of oxidative damage in the nucleus and cytosol. *Plant Cell Physiol.* 53:1596–1606. https://doi.org/10.1093/pcp/pcs100

Galluzzi, L., J.M. Bravo-San Pedro, O. Kepp, and G. Kroemer. 2016. Regulated cell death and adaptive stress responses. *Cell. Mol. Life Sci.* 73:2405–2410. https://doi.org/10.1007/s00018-016-2209-y

Galluzzi, L., I. Vitale, S.A. Aaronson, J.M. Abrams, D. Adam, P. Agostinis, E.S. Alnemri, L. Altucci, I. Amelio, D.W. Andrews, et al. 2018. Molecular mechanisms of cell death: recommendations of the Nomenclature Committee on Cell Death 2018. *Cell Death Differ.* 25:486–541. https://doi.org/10.1038/s41418-017-0012-4

Gumbo, J.R., T.E. Cloete, G.J.J. van Zyl, and J.E.M. Sommerville. 2014. The viability assessment of Microcystis aeruginosa cells after co-culturing with Bacillus mycoides B16 using flow cytometry. Physics and Chemistry of the Earth, Parts A/B/C. *Transboundary Water Cooperation: Building Partnerships.* 72–75:24–33. https://doi.org/10.1016/j.pce.2014.09.004

Hakem, R., A. Hakem, G.S. Duncan, J.T. Henderson, M. Woo, M.S. Soengas, A. Elia, J.L. de la Pompa, D. Kagi, W. Khoo, et al. 1998. Differential requirement for caspase 9 in apoptotic pathways in vivo. *Cell.* 94:339–352. https://doi.org/10.1016/S0092-8674(00)81477-4

Hansen, J., A. Garreta, M. Benincasa, M.C. Fusté, M. Busquets, and A. Manresa. 2013. Bacterial lipoxygenases, a new subfamily of enzymes? A phylogenetic approach. *Appl. Microbiol. Biotechnol.* 97:4737–4747. https://doi.org/10.1007/s00253-013-4887-9

Havaux, M. 2020. Plastoquinone In and Beyond Photosynthesis. *Trends Plant Sci.* 25:1252–1265. https://doi.org/10.1016/j.tplants.2020.06.011

Havaux, M., G. Guedeney, M. Hagemann, N. Yeremenko, H.C.P. Matthijs, and R. Jeanjean. 2005. The chlorophyll-binding protein IsiA is inducible by high light and protects the cyanobacterium Synechocystis PCC6803 from photooxidative stress. *FEBS Lett.* 579:2289–2293. https://doi.org/10.1016/j.febslet.2005.03.021

Henke, N., P. Albrecht, I. Bouchachia, M. Ryazantseva, K. Knoll, J. Lewerenz, E. Kaznacheyeva, P. Maher, and A. Methner. 2013. The plasma membrane channel ORAI1 mediates detrimental calcium influx caused by endogenous oxidative stress. *Cell Death Dis.* 4:e470. https://doi.org/10.1038/cddis.2012.216

Hernandez-Prieto, M.A., and M.E. Futschik. 2012. CyanoEXpress: A web database for exploration and visualisation of the integrated transcriptome of cyanobacterium Synechocystis sp. PCC6803. *Bioinformation.* 8:634–638. https://doi.org/10.6026/97320630008634

Hewelt-Belka, W., Á. Kot-Wasik, P. Tamagnini, and P. Oliveira. 2020. Untargeted Lipidomics Analysis of the Cyanobacterium *Synechocystis* sp. PCC 6803: Lipid Composition Variation in Response to Alternative Cultivation Setups and to Gene Deletion. *Int. J. Mol. Sci.* 21:8883. https://doi.org/10.3390/ijms21238883

Hu, C., and P. Rzymski. 2019. Programmed cell death-like and accompanying release of microcystin in freshwater bloom-forming cyanobacterium Microcystis: From identification to ecological relevance. *Toxins (Basel).* 11:E706. https://doi.org/10.3390/toxins11120706

Imai, H., M. Matsuoka, T. Kumagai, T. Sakamoto, and T. Koumura. 2017. Lipid peroxidation-dependent cell death regulated by GPx4 and ferroptosis. *Curr. Top. Microbiol. Immunol.* 403:143–170. https://doi.org/10.1007/82_2016_508

Johnson, L.A., and L.A. Hug. 2019. Distribution of reactive oxygen species defense mechanisms across domain bacteria. *Free Radic. Biol. Med.* 140:93–102. https://doi.org/10.1016/j.freeradbiomed.2019.03.032

Kaczmarzyk, D., and M. Fulda. 2010. Fatty acid activation in cyanobacteria mediated by acyl-acyl carrier protein synthetase enables fatty acid recycling. *Plant Physiol.* 152:1598–1610. https://doi.org/10.1104/pp.109.148007

Kagan, V.E., G. Mao, F. Qu, J.P.F. Angeli, S. Doll, C.S. Croix, H.H. Dar, B. Liu, V.A. Tyurin, V.B. Ritov, et al. 2017. Oxidized Arachidonic/Adrenic Phosphatidylethanolamines Navigate Cells to Ferroptosis. *Nat. Chem. Biol.* 13:81–90. https://doi.org/10.1038/nchembio.2238

Klemenčič, M., and C. Funk. 2018. Structural and functional diversity of caspase homologues in non-metazoan organisms. *Protoplasma.* 255:387–397. https://doi.org/10.1007/s00709-017-1145-5

Klemenčič, M., J. Asplund-Samuelsson, M. Dolinar, and C. Funk. 2019. Phylogenetic distribution and diversity of bacterial pseudo-orthocaspases underline their putative role in photosynthesis. *Front Plant Sci.* 10:293. https://doi.org/10.3389/fpls.2019.00293

Kopf, M., S. Klähn, I. Scholz, J.K.F. Matthiessen, W.R. Hess, and B. Voß. 2014. Comparative analysis of the primary transcriptome of Synechocystis sp. PCC 6803. *DNA Res.* 21:527–539. https://doi.org/10.1093/dnares/dsu018

Kroemer, G., L. Galluzzi, P. Vandenabeele, J. Abrams, E.S. Alnemri, E.H. Baehrecke, M.V. Blagosklonny, W.S. El-Deiry, P. Golstein, D.R. Green, et al. Nomenclature Committee on Cell Death 2009. 2009. Classification of cell death: recommendations of the Nomenclature Committee on Cell Death 2009. *Cell Death Differ.* 16:3–11. https://doi.org/10.1038/cdd.2008.150

Latifi, A., M. Ruiz, and C.-C. Zhang. 2009. Oxidative stress in cyanobacteria. *FEMS Microbiol. Rev.* 33:258–278. https://doi.org/10.1111/j.1574-6976.2008.00134.x

Lee, H.W., B.S. Park, J.-H. Joo, S.K. Patidar, H.J. Choi, E. Jin, and M.-S. Han. 2018. Cyanobacteria-specific algicidal mechanism of bioinspired naphthoquinone derivative, NQ 2-0. *Sci. Rep.* 8:11595. https://doi.org/10.1038/s41598-018-29976-5

Lenth, R.V. 2016. Least-Squares means: The R package lsmeans. *J. Stat. Softw.* 69:1–33. https://doi.org/10.18637/jss.v069.i01

Lindsten, T., A.J. Ross, A. King, W.X. Zong, J.C. Rathmell, H.A. Shiels, E. Ulrich, K.G. Waymire, P. Mahar, K. Frauwirth, et al. 2000. The combined functions of proapoptotic Bcl-2 family members bak and bax are essential for normal development of multiple tissues. *Mol. Cell.* 6: 1389–1399. https://doi.org/10.1016/S1097-2765(00)00136-2

Liu, M., and S. Lu. 2016. Plastoquinone and Ubiquinone in Plants: Biosynthesis, Physiological Function and Metabolic Engineering. *Front Plant Sci.* 7:1898. https://doi.org/10.3389/fpls.2016.01898

Maeda, H., Y. Sakuragi, D.A. Bryant, and D. Dellapenna. 2005. Tocopherols protect Synechocystis sp. strain PCC 6803 from lipid peroxidation. *Plant Physiol.* 138:1422–1435. https://doi.org/10.1104/pp.105.061135

Mao, C., X. Liu, Y. Zhang, G. Lei, Y. Yan, H. Lee, P. Koppula, S. Wu, L. Zhuang, B. Fang, et al. 2021. Author Correction: DHODH-mediated ferroptosis defence is a targetable vulnerability in cancer. *Nature.* 596:E13. https://doi.org/10.1038/s41586-021-03820-9

Meeks, J.C., and J. Elhai. 2002. Regulation of cellular differentiation in filamentous cyanobacteria in free-living and plant-associated symbiotic growth states. *Microbiol. Mol. Biol. Rev.* 66:94–121. https://doi.org/10.1128/MMBR.66.1.94-121.2002

Melino, G., R.A. Knight, and P. Nicotera. 2005. How many ways to die? How many different models of cell death? *Cell Death Differ.* 12(S2, Suppl 2): 1457–1462. https://doi.org/10.1038/sj.cdd.4401781

Minina, E.A., L.H. Filonova, K. Fukada, E.I. Savenkov, V. Gogvadze, D. Clapham, V. Sanchez-Vera, M.F. Suarez, B. Zhivotovsky, G. Daniel, et al. 2013. Autophagy and metacaspase determine the mode of cell death in plants. *J. Cell Biol.* 203:917–927. https://doi.org/10.1083/jcb.201307082

Müller-Schüssele, S.J., M. Schwarzländer, and A.J. Meyer. 2021. Live monitoring of plant redox and energy physiology with genetically encoded biosensors. *Plant Physiol.* 186:93–109. https://doi.org/10.1093/plphys/kiab019

Mullineaux, C.W. 2014. Co-existence of photosynthetic and respiratory activities in cyanobacterial thylakoid membranes. *Biochim. Biophys. Acta.* 1837:503–511. https://doi.org/10.1016/j.bbabio.2013.11.017

Nakajima, Y., Y. Umena, R. Nagao, K. Endo, K. Kobayashi, F. Akita, M. Suga, H. Wada, T. Noguchi, and J.-R. Shen. 2018. Thylakoid membrane lipid sulfoquinovosyl-diacylglycerol (SQDG) is required for full functioning of photosystem II in *Thermosynechococcus elongatus*. *J. Biol. Chem.* 293: 14786–14797. https://doi.org/10.1074/jbc.RA118.004304

Nara, T., T. Hshimoto, and T. Aoki. 2000. Evolutionary implications of the mosaic pyrimidine-biosynthetic pathway in eukaryotes. *Gene.* 257: 209–222. https://doi.org/10.1016/S0378-1119(00)00411-X

Narainsamy, K., S. Farci, E. Braun, C. Junot, C. Cassier-Chauvat, and F. Chauvat. 2016. Oxidative-stress detoxification and signalling in cyanobacteria: the crucial glutathione synthesis pathway supports the production of ergothioneine and ophthalmate. *Mol. Microbiol.* 100: 15–24. https://doi.org/10.1111/mmi.13296

Noctor, G., A. Mhamdi, S. Chaouch, Y. Han, J. Neukermans, B. Marquez-Garcia, G. Queval, and C.H. Foyer. 2012. Glutathione in plants: an integrated overview. *Plant Cell Environ.* 35:454–484. https://doi.org/10.1111/j.1365-3040.2011.02400.x

Ozgur, R., I. Turkan, B. Uzilday, and A.H. Sekmen. 2014. Endoplasmic reticulum stress triggers ROS signalling, changes the redox state, and regulates the antioxidant defence of Arabidopsis thaliana. *J. Exp. Bot.* 65: 1377–1390. https://doi.org/10.1093/jxb/eru034

Pérez-Pérez, M.E., E. Martín-Figueroa, and F.J. Florencio. 2009. Photosynthetic regulation of the cyanobacterium Synechocystis sp. PCC 6803 thioredoxin system and functional analysis of TrxB (Trx x) and TrxQ (Trx y) thioredoxins. *Mol. Plant.* 2:270–283. https://doi.org/10.1093/mp/ssn070

Rajaram, H., A.K. Chaurasia, and S.K. Apte. 2014. Cyanobacterial heat-shock response: role and regulation of molecular chaperones. *Microbiology (Reading).* 160:647–658. https://doi.org/10.1099/mic.0.073478-0

Ren, H., X. Zhao, W. Li, J. Hussain, G. Qi, and S. Liu. 2021. Calcium Signaling in Plant Programmed Cell Death. *Cells.* 10:1089. https://doi.org/10.3390/cells10051089

Rippka, R., J. Deruelles, J.B. Waterbury, M. Herdman, and R.Y. Stanier. 1979. Generic assignments, strain histories and properties of pure cultures of Cyanobacteria. *Microbiology.* 111:1–61. https://doi.org/10.1099/00221287-111-1-1

Ristic, Z., U. Bukovnik, and P.V.V. Prasad. 2007. Correlation between Heat Stability of Thylakoid Membranes and Loss of Chlorophyll in Winter Wheat under Heat Stress. *Crop Sci.* 47:2067–2073. https://doi.org/10.2135/cropsci2006.10.0674

Saraste, A., and K. Pulkki. 2000. Morphologic and biochemical hallmarks of apoptosis. *Cardiovasc. Res.* 45:528–537. https://doi.org/10.1016/S0008-6363(99)00384-3

Schulze, K., D.A. López, U.M. Tillich, and M. Frohme. 2011. A simple viability analysis for unicellular cyanobacteria using a new autofluorescence assay, automated microscopy, and ImageJ. *BMC Biotechnol.* 11:118. https://doi.org/10.1186/1472-6750-11-118

Seibt, T.M., B. Proneth, and M. Conrad. 2019. Role of GPX4 in ferroptosis and its pharmacological implication. *Free Radic. Biol. Med.* 133:144–152. https://doi.org/10.1016/j.freeradbiomed.2018.09.014

Seiler, A., M. Schneider, H. Förster, S. Roth, E.K. Wirth, C. Culmsee, N. Plesnila, E. Kremmer, O. Rådmark, W. Wurst, et al. 2008. Glutathione peroxidase 4 senses and translates oxidative stress into 12/15-lipoxygenase dependent- and AIF-mediated cell death. *Cell Metab.* 8:237–248. https://doi.org/10.1016/j.cmet.2008.07.005

Sharathchandra, K., and M. Rajashekhar. 2011. Total lipid and fatty acid composition in some freshwater cyanobacteria. *J. Algal Biomass Util.* 2: 83–97.

Singh, S., R. Sinha, and D. Hader. 2002. Role of lipids and fatty acids in stress tolerance in cyanobacteria. *Acta Protozool.* 41:297–308.

Skouta, R., S.J. Dixon, J. Wang, D.E. Dunn, M. Orman, K. Shimada, P.A. Rosenberg, D.C. Lo, J.M. Weinberg, A. Linkermann, and B.R. Stockwell. 2014. Ferrostatins inhibit oxidative lipid damage and cell death in diverse disease models. *J. Am. Chem. Soc.* 136:4551–4556. https://doi.org/10.1021/ja411006a

Spungin, D., K.D. Bidle, and I. Berman-Frank. 2019. Metacaspase involvement in programmed cell death of the marine cyanobacterium Trichodesmium. *Environ. Microbiol.* 21:667–681. https://doi.org/10.1111/1462-2920.14512

Stockwell, B.R., and X. Jiang. 2020. The Chemistry and Biology of Ferroptosis. *Cell Chem. Biol.* 27:365–375. https://doi.org/10.1016/j.chembiol.2020.03.013

Stockwell, B.R., J.P. Friedmann Angeli, H. Bayir, A.I. Bush, M. Conrad, S.J. Dixon, S. Fulda, S. Gascón, S.K. Hatzios, V.E. Kagan, et al. 2017. Ferroptosis: a regulated cell death nexus linking metabolism, redox biology, and disease. *Cell.* 171:273–285. https://doi.org/10.1016/j.cell.2017.09.021

Suginaka, K., K. Yamamoto, H. Ashida, Y. Sawa, and H. Shibata. 1999. Effect of intracellular glutathione on heat-induced cell death in the cyanobacterium, Synechocystis PCC 6803. *Biosci. Biotechnol. Biochem.* 63: 1112–1115. https://doi.org/10.1271/bbb.63.1112

Sun, W.-Y., V.A. Tyurin, K. Mikulska-Ruminska, I.H. Shrivastava, T.S. Anthonymuthu, Y.-J. Zhai, M.-H. Pan, H.-B. Gong, D.-H. Lu, J. Sun, et al. 2021. Phospholipase iPLA$_2$β averts ferroptosis by eliminating a redox lipid death signal. *Nat. Chem. Biol.* 17:465–476. https://doi.org/10.1038/s41589-020-00734-x

Swapnil, P., A.K. Yadav, S. Srivastav, N.K. Sharma, S. Srikrishna, and A.K. Rai. 2017. Biphasic ROS accumulation and programmed cell death in a cyanobacterium exposed to salinity (NaCl and Na2SO4). *Algal Res.* 23: 88–95. https://doi.org/10.1016/j.algal.2017.01.014

Tiwari, A., P. Singh, and R.K. Asthana. 2016. Role of calcium in the mitigation of heat stress in the cyanobacterium Anabaena PCC 7120. *J. Plant Physiol.* 199:67–75. https://doi.org/10.1016/j.jplph.2016.05.012

Torrecilla, I., F. Leganés, I. Bonilla, and F. Fernández-Piñas. 2000. Use of recombinant aequorin to study calcium homeostasis and monitor calcium transients in response to heat and cold shock in cyanobacteria. *Plant Physiol.* 123:161–176. https://doi.org/10.1104/pp.123.1.161

Torrecilla, I., F. Leganés, I. Bonilla, and F. Fernández-Piñas. 2004. A calcium signal is involved in heterocyst differentiation in the cyanobacterium

Anabaena sp. PCC7120. *Microbiology (Reading)*. 150:3731–3739. https://doi.org/10.1099/mic.0.27403-0

Tyurin, V.A., Y.Y. Tyurina, P.M. Kochanek, R. Hamilton, S.T. DeKosky, J.S. Greenberger, H. Bayir, and V.E. Kagan. 2008. Oxidative lipidomics of programmed cell death. *Methods Enzymol.* 442:375–393. https://doi.org/10.1016/S0076-6879(08)01419-5

Tyurina, Y.Y., R.M. Domingues, V.A. Tyurin, E. Maciel, P. Domingues, A.A. Amoscato, H. Bayir, and V.E. Kagan. 2014. Characterization of cardiolipins and their oxidation products by LC-MS analysis. *Chem. Phys. Lipids*. 179:3–10. https://doi.org/10.1016/j.chemphyslip.2013.12.003

Van Hautegem, T., A.J. Waters, J. Goodrich, and M.K. Nowack. 2015. Only in dying, life: programmed cell death during plant development. *Trends Plant Sci.* 20:102–113. https://doi.org/10.1016/j.tplants.2014.10.003

Van Opdenbosch, N., and M. Lamkanfi. 2019. Caspases in cell death, inflammation and disease. *Immunity*. 50:1352–1364. https://doi.org/10.1016/j.immuni.2019.05.020

von Berlepsch, S., H.-H. Kunz, S. Brodesser, P. Fink, K. Marin, U.-I. Flügge, and M. Gierth. 2012. The acyl-acyl carrier protein synthetase from Synechocystis sp. PCC 6803 mediates fatty acid import. *Plant Physiol.* 159:606–617. https://doi.org/10.1104/pp.112.195263

Wada, H., and N. Murata. 1998. Membrane Lipids in Cyanobacteria. *In* Lipids in Photosynthesis: Structure, Function and Genetics, Advances in Photosynthesis and Respiration. S. Paul-André, and M. Norio, editors. Springer Netherlands, Dordrecht. 65–81., https://doi.org/10.1007/0-306-48087-5_4

Whitton, B. 2012. Ecology of Cyanobacteria II. Springer, The Netherlands. https://doi.org/10.1007/978-94-007-3855-3

Yalcintepe, L., and E. Halis. 2016. Modulation of iron metabolism by iron chelation regulates intracellular calcium and increases sensitivity to doxorubicin. *Bosn. J. Basic Med. Sci.* 16:14–20. https://doi.org/10.17305/bjbms.2016.576

Yang, W.S., and B.R. Stockwell. 2016. Ferroptosis: Death by Lipid Peroxidation. *Trends Cell Biol.* 26:165–176. https://doi.org/10.1016/j.tcb.2015.10.014

Yang, W.S., R. SriRamaratnam, M.E. Welsch, K. Shimada, R. Skouta, V.S. Viswanathan, J.H. Cheah, P.A. Clemons, A.F. Shamji, C.B. Clish, et al. 2014. Regulation of ferroptotic cancer cell death by GPX4. *Cell.* 156:317–331. https://doi.org/10.1016/j.cell.2013.12.010

Yang, W.S., K.J. Kim, M.M. Gaschler, M. Patel, M.S. Shchepinov, and B.R. Stockwell. 2016. Peroxidation of polyunsaturated fatty acids by lipoxygenases drives ferroptosis. *Proc. Natl. Acad. Sci. USA.* 113:E4966–E4975. https://doi.org/10.1073/pnas.1603244113

Yang, J., X.-Q. Chai, X.-X. Zhao, and X. Li. 2017. Comparative genomics revealed the origin and evolution of autophagy pathway. *J. Syst. Evol.* 55:71–82. https://doi.org/10.1111/jse.12212

Yang, W., F. Wang, L.-N. Liu, and N. Sui. 2020. Responses of Membranes and the Photosynthetic Apparatus to Salt Stress in Cyanobacteria. *Front Plant Sci.* 11:713. https://doi.org/10.3389/fpls.2020.00713

Yoshida, H., Y.Y. Kong, R. Yoshida, A.J. Elia, A. Hakem, R. Hakem, J.M. Penninger, and T.W. Mak. 1998. Apaf1 is required for mitochondrial pathways of apoptosis and brain development. *Cell.* 94:739–750. https://doi.org/10.1016/S0092-8674(00)81733-X

Zheng, W., U. Rasmussen, S. Zheng, X. Bao, B. Chen, Y. Gao, X. Guan, J. Larsson, and B. Bergman. 2013. Multiple Modes of Cell Death Discovered in a Prokaryotic (Cyanobacterial) Endosymbiont. *PLoS One.* 8:e66147. https://doi.org/10.1371/journal.pone.0066147

Zhou, B., J. Liu, R. Kang, D.J. Klionsky, G. Kroemer, and D. Tang. 2020a. Ferroptosis is a type of autophagy-dependent cell death. *Semin. Cancer Biol.* 66:89–100. https://doi.org/10.1016/j.semcancer.2019.03.002

Zhou, T., H. Cao, J. Zheng, F. Teng, X. Wang, K. Lou, X. Zhang, and Y. Tao. 2020b. Suppression of water-bloom cyanobacterium Microcystis aeruginosa by algaecide hydrogen peroxide maximized through programmed cell death. *J. Hazard. Mater.* 393:122394. https://doi.org/10.1016/j.jhazmat.2020.122394

Zuppini, A., C. Andreoli, and B. Baldan. 2007. Heat stress: an inducer of programmed cell death in Chlorella saccharophila. *Plant Cell Physiol.* 48:1000–1009. https://doi.org/10.1093/pcp/pcm070

Supplemental material

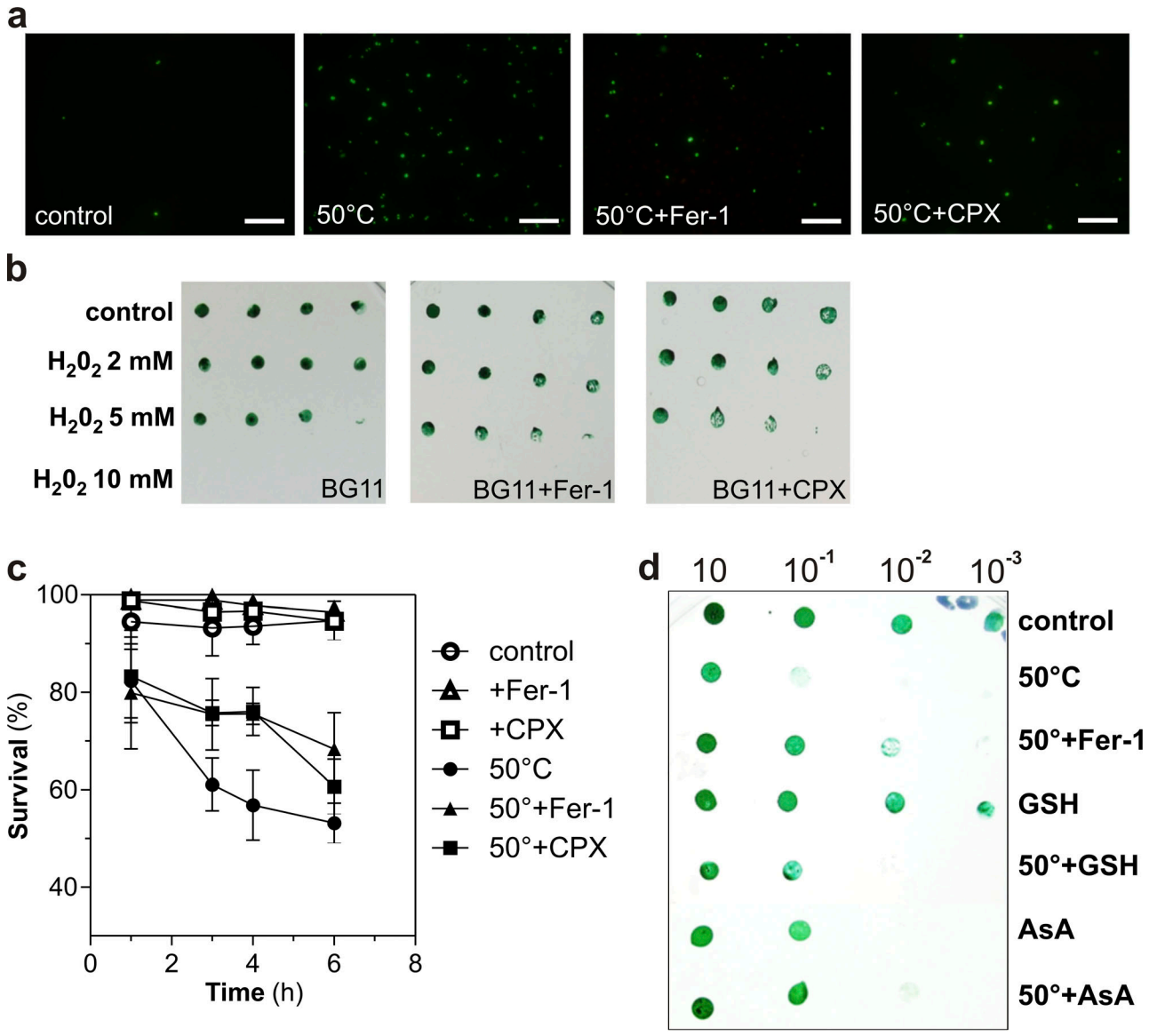

Figure S1. **Viability assays. (a)** Representative fluorescence images showing cell death in *Synechocystis* sp. PCC 6803 detected by SYTOX Green nucleic acid stain. **(b)** Neither Fer-1 nor CPX prevented cell death triggered by H_2O_2 treatments. **(c)** Kinetics of cell death induced by 50°C. **(d)** GSH (100 µM) and AsA (1 µM) addition prevents cell death induced by 50°C HS (10 min). **(a–d)** Cultures were preincubated with DMSO, Fer-1 (1 µM), or CPX (1 µM) for 24 h before HS. **(b and d)** Viability was tested via drop test. Scale bars, 5 µm.

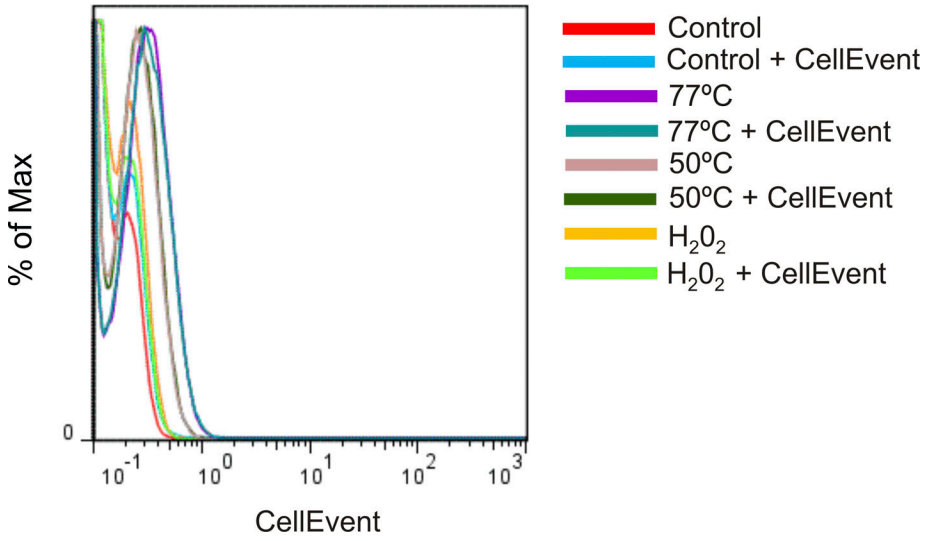

Figure S2. **Caspase-like activity measured by flow cytometry using CellEvent after 50°C, 77oC for 10 min, or with H_2O_2 10 mM for 1 h.**

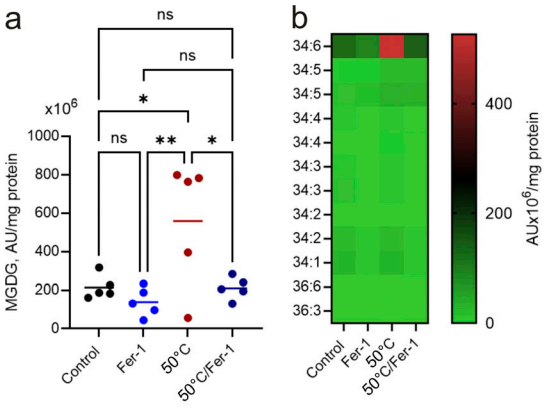

c

MGDG species identified in cyanobacteria

MGDG	m/z	error, ppm	Suggested species
MGDG (34:6)	805.5108	1.76	16:3-18:3
MGDG (34:5)	807.5264	1.80	16:3-18:2
MGDG (34:5)	807.5264	0.78	16:2-18:3
MGDG (34:4)	809.5420	-0.78	16:1-18:2
MGDG (34:4)	809.5420	-7.75	16:0-18:3
MGDG (34:3)	811.5577	-3.03	16:1-18:2
MGDG (34:3)	811.5577	-2.34	16:0-18:3
MGDG (34:2)	813.5734	-4.83	16:1-18:1
MGDG (34:2)	813.5734	-2.34	16:0-18:2
MGDG (34:1)	815.5889	-2.33	16:0-18:1
MGDG (36:6)	835.5575	1.94	18:3-18:3
MGDG (36:3)	839.5889	-5.13	18:1-18:2

No oxygenated MGDG species were detected.

Figure S3. **Content of MGDG species in cyanobacteria.** Data are presented as pmol/mg protein. Statistic: one-way ANOVA. Separation and quantification of lipid was performed by using reverse phase chromatography. MGDG species were detected as acetate adducts. *, P < 0.05 versus control; **, P < 0.05 versus ΔwspF (one-way ANOVA); *n* = 5.

One table is provided online as a separate file. Table S1 shows primers used in this study in qPCR reactions.